AN ANALYSIS OF MULTI-FREQUENCY CARRIER PHASE LINEAR COMBINATIONS FOR GNSS

LANDON URQUHART

February 2009

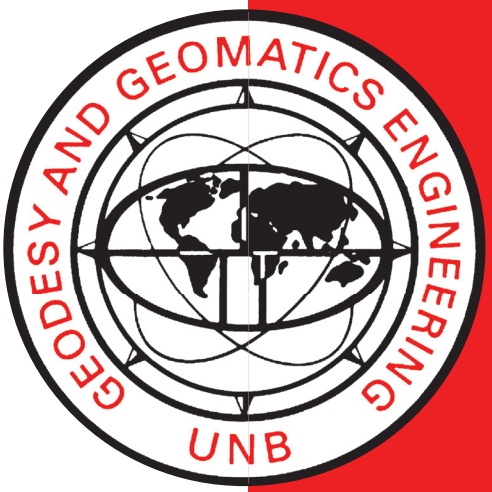

TECHNICAL REPORT
NO. 263

AN ANALYSIS OF MULTI-FREQUENCY CARRIER PHASE LINEAR COMBINATIONS FOR GNSS

Landon Urquhart

Department of Geodesy and Geomatics Engineering
University of New Brunswick
P.O. Box 4400
Fredericton, N.B.
Canada
E3B 5A3

February 2009

PREFACE

This technical report is a reproduction of an undergraduate senior technical report submitted in partial fulfillment of the requirements for the degree of Bachelor of Science in Engineering in the Department of Geodesy and Geomatics Engineering, April 2008 and subsequently revised. The research was supervised by Dr. Marcelo Santos and partially funded by the Natural Sciences and Engineering Research Council of Canada.

As with any copyrighted material, permission to reprint or quote extensively from this report must be received from the author. The citation to this work should appear as follows:

Urquhart, L. (2009). *An Analysis of Multi-Frequency Carrier Phase Linear Combinations for GNSS*. Senior technical report, Department of Geodesy and Geomatics Engineering Technical Report No. 263, University of New Brunswick, Fredericton, New Brunswick, Canada, 71 pp.

ABSTRACT

With the modernization of GPS and the deployment of Galileo expected soon, there will be an increase in the number of precise or carrier phase signals arriving from space which are at our disposal. One method of utilizing these signals is to form carrier phase linear combinations which: 1) reduce ionospheric delay; 2) reduce receiver noise; 3) increase the wavelength of the observable. This means improved position capability and more reliability for these space based systems.

This report focuses its investigation on those combinations which mitigate ionospheric delay, reduce receiver noise and perform best under typical survey conditions. The derivation of the characteristics for the linear combinations is performed including the second and third order ionosphereic delay amplification factors.

A number of conclusions are reached. It is possible to more effectively reduce the effect of the ionosphere by using three frequencies rather than two frequencies. Care must be taken in understanding the effects of the linear combinations on the higher order terms especially for very precise applications. Concerning receiver noise, it was shown theoretically that although the triple frequency narrow-lane combination does improve the precision of the measurement it is more effective to use the three frequencies independently to improve the precision in the position domain.

Finally it was shown through the use of simulated modernized GPS observations that linear combinations can be very effective in reducing the errors present in satellite positioning.

ACKNOWLEDGEMENTS

I would like to take this time to thank those that have contributed to my work. Firstly, I would like to thank Dr. Marcelo Santos for being my supervisor and providing me with my topic. Additionally, he was very gracious to listen to my questions and explain any difficulties I had understanding GPS. As well I must thank the University of Calgary for supplying me with the simulation program to allow me to analyze the data. I would like to thank Dr. Lachapelle for his assistance in answering my questions concerning the simulation program. Finally, I would like to thank NSERC for providing funding for a summer research position that provided me the opportunity to carry out this research.

TABLE OF CONTENTS

LIST OF FIGURES

LIST OF TABLES

1.0 INTRODUCTION

In 1983, a prediction:
"… postulate the limit of this evolution: a cheap "wrist locator" giving instantaneous positions to an accuracy of 1 mm."
"One day, perhaps 100 years from now, the wrist locator will exist"

- Petr Vanicek, extract from [Santos, 2003]

Although millimetre positioning may still be a long way off, steps are currently underway to improve the achievable accuracy of satellite positioning. To improve the current Global Positioning System (GPS) the Department of Defense (DoD) has begun to execute a modernization program that includes an improvement of the current L2 frequency as well as the addition of a third frequency. Additionally, the European Union (EU) has begun the deployment of the Galileo system that will also contain three frequencies available to all users of the system. Once fully deployed, these systems will provide users with six carrier phase observations to be used in precise positioning applications.

GPS satellites as well as those being developed for Galileo will have both code and carrier phase observables. Although the code observables are adequate for many every day positioning or navigation needs, high precision satellite positioning requires the use of carrier phase measurements. With this comes an added complexity of the receiver only being capable of measuring the fraction of a cycle and how many cycles have passed since the receiver gained lock. It is necessary to solve for this carrier phase ambiguity which results from the receiver not knowing how many cycles of the carrier wave exist between the satellite and the receiver.

Forming linear combinations of the carrier phase observations can eliminate or at least reduce the effect of biases and noise which can hamper precise positioning. With the

introduction of a third GPS frequency, as well as Galileo there will be added benefit to forming these combinations in the achievable reduction of these biases and noise. This will improve ambiguity resolution as well as the overall positioning result.

There are an infinite number of linear combinations that mitigate errors present in satellite positioning. This report investigates the optimal linear combinations of multi-frequency carrier phase observations to improve the overall accuracy and precision of satellite positioning. Before we take an in depth look at the motivation behind using linear combinations of carrier phase observations a brief look at the characteristics of the GPS and Galileo signals is necessary.

1.2 GNSS SIGNAL CHARACTERISTICS

The US has begun a program to modernize the current GPS. The goal of this program is to improve signal quality and reliability thereby increasing the applications of GPS. Some examples of these applications include indoor positioning and aircraft navigation [Fontana et al., 2001]. These improved signals will be more robust, have higher signal to noise values and have greater protection against interference than the current system. If the program remains on track the system should have full capability by 2015, although the program is already behind schedule [Rizos et al., 2005].

Currently, GPS satellites transmit on two carrier frequencies, L1 at 1575.42 MHz and L2 at 1227.60 MHz. The L1 frequency consists of two pseudorandom noise codes, the C/A and P code, while currently on the L2 frequency only the P code is available for use by civil users. The first step of the modernization program is to add a C/A code to the L2 frequency to allow civil users to better account for ionospheric refraction, have higher signal to noise ratio

and be less susceptible to multipath [Rizos et al., 2005]. Table 1.1 shows the satellites that currently broadcast the L2C signal. Work has already been done to show the benefits of the L2C signal relating to acquisition strength and signal-to-noise ratio (see Sükeová et al., 2007).

Table 1.1 Satellites Broadcasting L2C Signal, as of August 2008

Satellite	PRN-7	PRN-12	PRN-15	PRN-17	PRN-29	PRN-31
Date of Launch	15/03/08	17/11/06	17/10/07	26/09/05	20/12/07	25/09/06

One issue with the L2 signal is that it is not in the Aeronautical Radionavigation/Satellite Service (ARS) band [Department of Defence and Department of Transportation, 2001]. This means that it is not applicable for aeronautical applications that require *safety-of-life* standards. The addition of the new L5 signal, transmitting at 1176.45 MHz, will have a large impact on the aeronautical community because it is within the ARS band allowing aeronautical users to benefit from the use of dual frequency positioning by removing the first order ionospheric delay. An initial look at the L5 signal was expected during the summer of 2008 but this has been pushed back due to concerns with the launch vehicle [Inside GNSS, 2008]. Table 1.2 shows the characteristics of the three GPS signals.

Table 1.2 Characteristics of GPS Signals

GPS	Freq. (Mhz)	Wavelength(m)
L1	1575.42	0.1903
L2	1227.6	0.2442
L5	1176.45	0.2548

In addition to the modernization of GPS, the EU's Galileo program is likely to have a huge impact on satellite positioning in the future. Although there have been issues with funding, a new agreement among the EU to publicly fund the program could mean that the

constellation will be operational as soon as 2013, although the past track record would imply that this is very optimistic [Inside GNSS, 2007]. The constellation will consist of 27 fully operational satellites and three replacements. Each Galileo satellite will broadcast 10 navigation signals, on four frequencies. Figure 1.1 shows the location of both the Galileo and GPS signals in the radio spectrum.

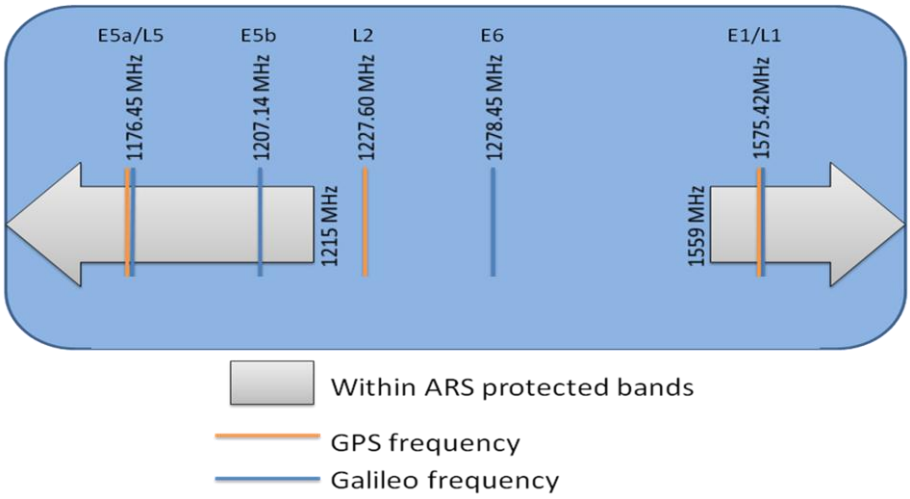

Figure 1.1 Location of GPS and Galileo Signals in Radio Spectrum

With the variety of signals it will be possible for Galileo to provide open, safety-of-life, commercial and public regulated services. This will provide users with a variety of schemes to fit their needs. Table 1.3 summarizes the Galileo signals.

Table 1.3 Characteristics of Galileo Signals

GALILEO	Freq. (Mhz)	Wavelength(m)	Service
E1	1575.42	0.1903	open
E6	1278.42	0.2345	closed
E5a	1176.45	0.2548	open
E5b	1207.14	0.2483	open

As for the current status of the constellation the first two Galileo test satellites have

been launched and tested successfully. The third launch is scheduled for late 2008 [ESA, 2007]. In this analysis only the open frequencies are considered since these will be freely available to all users.

1.3 MOTIVATION FOR LINEAR COMBINATIONS

Now that we are more familiar with the two systems we can move on to the motivation of using linear combinations of carrier phase observations. Linear combinations are most often used for three purposes: 1) The final combination is a wide-lane, with a wavelength greater than L5 or E5a; 2) The effect of the ionosphere is reduced compared to that on the L1 and E1 frequency; 3) The noise and multipath of the combination is reduced compared to that on L1 or E1 frequencies.

Forming a wide-lane observable has many advantages for ambiguity resolution. By using the wide-lane it reduces the computational burden on the receiver by reducing the number of possible candidates for ambiguity resolution, thus reducing the search time.

By using linear combinations to reduce or eliminate unwanted terms in the observation equation we can improve the accuracy and precision of satellite positioning. An example of this is the ionosphere free combination which is currently used for single receiver positioning as well as for differential positioning if the length of the baseline prevents the use of double differencing to eliminate the ionospheric delay. One drawback with the ionosphere free combination is that it typically reduces the wavelength which complicates ambiguity resolution.

The third benefit of linear combinations is that it is possible to reduce the noise and multipath of the observation. This improves the precision of the final solution. In doing so, it also reduces the wavelength of the observable. This can be important for real time applications

such as network real-time kinematic (RTK) GPS or cellular applications which have limited bandwidth [Richert and El-Sheimy, 2007].

Like most things in life, with advantages come drawbacks. The same applies for linear combinations. In a perfect world we would look for combinations which have all of the desirable characteristics, that is, a combination that is a wide-lane, reduces receiver noise and reduces ionospheric refraction. This is represented by the green area in Figure 1.2 which would be an ideal combination.

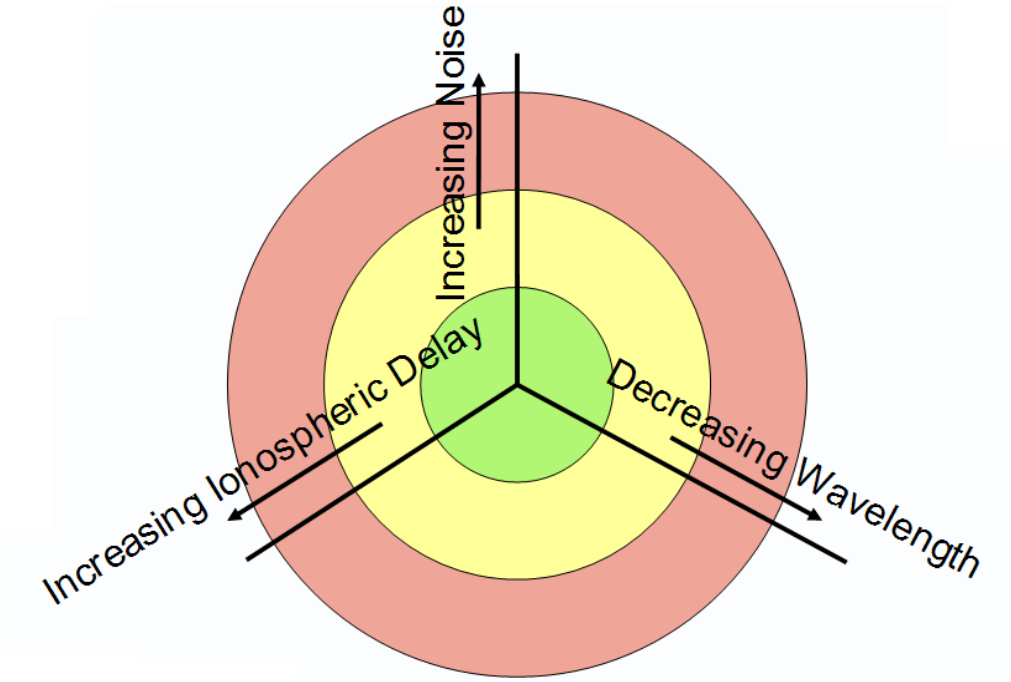

Figure 1.2 Balancing benefits and drawbacks of linear combinations

In the real world, we are often required to make sacrifices in one area to achieve the desired result in another. Depending on the conditions present in the field this means that the optimal combination will not always be the same.

Linear combinations of carrier phase observations are not a new concept in satellite positioning and their use is already an important aspect of current dual-frequency positioning

schemes. Cocard and Geiger [1992] perform an extensive search for all possible wide-lane combinations to be used for ambiguity resolution. Han and Rizos [1996] in an attempt to improve the Ambiguity Functional Method (AFM) for differential GPS describe optimal dual-frequency combinations for reducing the search space of the AFM. Collins [1999] builds on Cocard and Geiger's work and performs a comprehensive search for all possible linear combinations. Finally, Radovanovic [2002] outlines the criteria for an optimal linear combination to be used for kinematic positioning and then compares the results to the typical combinations used for dual-frequency positioning to the optimal choice.

Linear combinations have also been studied for multi-frequency GNSS. Han and Rizos [1999] build on their paper on dual-frequency combinations and look at ionosphere free and wide-lane combinations to assist with ambiguity resolution for triple frequency combinations. Odjick [2003] studies ionosphere free combinations of multi-frequency positioning and shows that by adding a third frequency it drastically increases the number of ionosphere free combinations which can be formed. The results are then quantified by ambiguity resolution success rate. Richert [2007] studies the optimal combination for differential positioning for GPS and Galileo. These optimal combinations are determined by studying the ambiguity resolution and precision of the resultant position. Henkel and Günther [2007] follow Collins [1999] approach and describe linear combinations, for Galileo, and how they can improve ambiguity resolution. Finally, Cocard et al. [2008] applies the same principles to triple frequency combinations for GPS and introduces the concept of lane number to unambiguously describe the wavelength of a combination.

As can be seen from the extensive list of references above there are many reasons for using linear combinations. The next section will describe how this report expands on the past research and how an optimal linear combination will be selected.

1.4 METHODOLOGY

There are two methods which can be used in identifying optimal linear combinations. The more common approach is the **direct approach**. For this approach all possible combinations of the carrier frequencies are studied. The characteristics of the combinations are then compiled and those combinations which exhibit desirable characteristics are chosen. To implement this approach the combinations must be predefined and therefore do not adapt well to dynamic environments. The advantage to this approach is that it is less demanding computationally. This approach can be seen in Cocard et al. (2008) , Han and Rizos (1996) and Han (1999) among others.

Alternatively, in the **inverse approach** the coefficients that multiply each frequency, that we will call [i,j,k], are thought of as unknowns and are solved for using a minimization approach. This is similar to the Z-transformation for decorrelating ambiguities described in Teunnison (1995) and is the approach used in the automation of a gantry crane steering system outlined in Kim and Langley (2003). The advantage of this approach is that the optimal linear combination can adapt to various environments where the magnitude of the error sources will vary with time. The one disadvantage of this approach is that it can be very demanding computationally.

In this report the direct approach is used. This is done to clearly show the characteristics of each individual combination. As well the reduction of the computations is also desirable as will be seen in the section on ambiguity resolution. Further discussion on the inverse approach will be seen in the section on future work.

To identify the optimal linear combination of carrier phase observations this report will first discuss the error sources present for GNSS which can be mitigated or eliminated through

the use of linear combinations. Next, the derivation of the triple frequency linear combinations for both GPS and Galileo will be performed following the approach taken in Cocard et al. [2008]. Following this, tables will be compiled which show the optimal combinations for each the wide-lane, narrow-lane and reduced ionosphere criterion and a discussion on their properties will ensue. Additionally, an optimal combination for a typical positioning campaign with all errors present will be derived. Finally, an analysis will be done using simulated GNSS measurements to verify the choice of the optimal combination for each criterion.

This report diverges from many of the past studies by placing less focus on the ambiguity domain and more on measurement accuracy. The reasoning behind this approach is that there is no advantage to improved ambiguity resolution if it does not improve the overall accuracy. Richert [2007] also follows this methodology but the results are focused in the position domain rather than the measurement domain. By focusing on the measurement domain it will eliminate any bias that may result from the choice of ambiguity resolution technique. We will also be able to see the absolute effect of each combination on the range measurement.

We will begin our look at linear combinations by first discussing the background to satellite positioning and the errors present (Chapter 2). Next we will look at the derivation of the characteristics of triple frequency combinations (Chapter 3). Chapter 4 reviews the creation of the simulated data that is used in analyzing the combinations. The analysis of the selected combinations and final choice of an optimal combination will be seen in Chapter 5. Finally we will conclude with our summary and recommendations in Chapter 6.

2.0 BACKGROUND

Before we can begin our look at linear combinations of carrier phase observations a brief review of the error sources present in satellite positioning will be given. Additionally, ambiguity resolution and the role of the wide-lane combination will be discussed.

2.1 ERROR SOURCES FOR GNSS POSITIONING

In order to understand how we can improve the accuracy of satellite positioning it is first necessary to review the sources of error that are present. Below is a detailed description of the error sources that can be reduced using linear combinations and a brief summary of the other sources of error which are present in satellite positioning. The expected magnitude and possible mitigation techniques are described as well.

2.1.1 IONOSPHERIC REFRACTION

The ionosphere can be one of the major factors which limit the accuracy of satellite positioning. Normally, the ionosphere is described as the various layers of the atmosphere extending from 50-1000 km as is shown in Figure 2.1 [Komjathy, 1997]. When radio signals pass through these layers they are refracted. The refraction is a function of the Total Electron Content (TEC) present in the path of the signal and can cause vertical range errors on the order of 22 metres [Klobuchar, 1996].

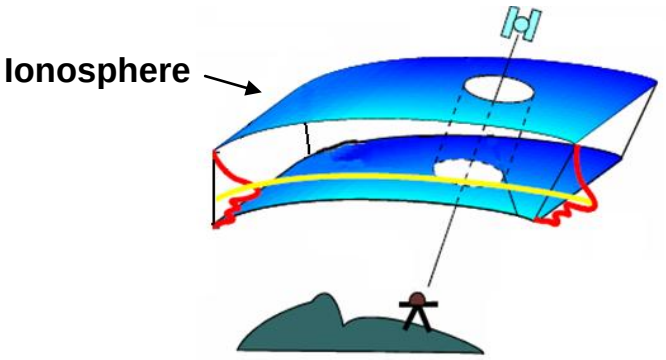

Figure 2.1 Propagation of GNSS signal through ionosphere [after Komjathy, 1997]

Because the ionosphere is dispersive to radio signals, which includes GNSS signals, it is possible to approximate the phase refractive index using the multiple frequencies. Following Seeber [1993] we have:

$$n_{ph} = 1 + \frac{c_2}{f^2} + \frac{c_3}{f^3} + \frac{c_4}{f^4} + \ldots \tag{2.1}$$

Currently, by combining L1 and L2 observables we can eliminate the ionospheric refraction by using the first order approximation of the refractive index. This eliminates the majority of the ionospheric delay but for very high precision applications or when solar activity is at a maximum there is still some residual error remaining. The ionospheric delay experienced by a GPS signal propagating through the ionosphere, including its higher order terms, can be expressed as [Bassiri and Haji, 1993]:

$$I_n = \left[\frac{Q}{f_n^2} + \frac{S}{2 f_n^3} + \frac{R}{3 f_n^4} \right], \tag{2.2}$$

where

$$\begin{aligned} Q &\approx 40.3 \int N \cdot dl \approx 40.3 TEC \\ S &= 7527 c \int N B_0 \left| \cos \theta_B \right| dl \\ R &= 2437 \int N^2 dl + 4.74 \cdot 10^{22} \int N B_0^2 (1 + \cos^2 \theta_B) dl \end{aligned} \quad ,$$

and N is the electron density, B_0 is the quantity of the earth's magnetic field and θ is the angle between the incoming signal and B_0.

With the introduction of triple frequency systems it will be possible to further eliminate the effect of the ionosphere by combining the three frequencies to form a second order approximation of the refractive index. Other options for dealing with ionospheric delay is to use differential positioning with a short baselines (approximately >10 km) and then double differencing between the two receivers and two satellites.

2.1.2 THERMAL NOISE

As with all electronic devices, GNSS receivers all contain some noise. The amount of noise, which is a stochastic error, is dependent on the type and quality of the receiver. With most of the newer GNSS receivers this error is on the order of 1% of the wavelength or better [Misra and Enge, 2001]. All of the components of a receiver, the antenna, amplifiers and cables contribute to this noise which is in the band of the signal of interest. Additionally, the signal strength and elevation angle of the satellite will have an effect on the noise present in the receiver.

Since thermal noise is a stochastic error we can not model it. To reduce it we can use linear combinations or we can combine the three frequencies independently [Petovello, 2006].

2.1.3 MULTIPATH

Multipath occurs when signals from a satellite arrive at the receiver multiple times. This is usually caused by the reflection of the signal from nearby buildings or objects that is shown in Figure 2.2.

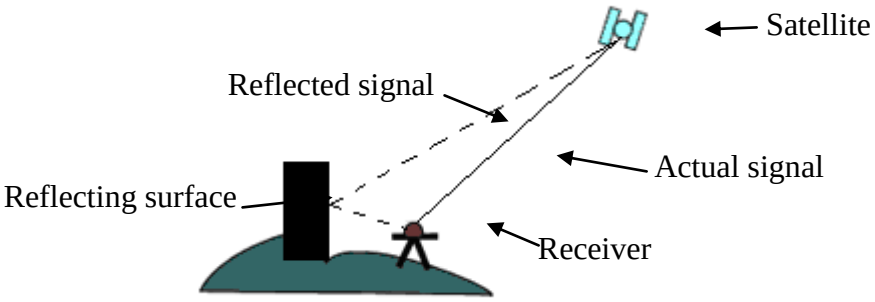

Figure 2.2 *Occurrence of multipath on a GNSS signal*

Hoffman-Wellenhof et al. [2001] shows that the maximum value for multipath is one quarter of the wavelength of the signal. For the carrier wave this translates to a maximum error of approximately 5 cm, depending on which frequency is used.

There are many options for reducing multipath. These include choosing locations that are not likely to have reflective surfaces, using proper antennae and setting proper elevation angle cutoffs. Of these choices the obvious solution is to select sites that are not inclined to multipath. However, as the applications of satellite positioning grow there are more demands for eliminating the effect of multipath as we move into harsher environments such as urban canyons.

Depending on the application multipath can be thought of as a systematic error or a pseudo-random error. In either case combinations that reduce noise often reduce multipath as well. For this reason a separate analysis into combinations that reduce multipath will not be done for this report.

2.1.4 OTHER SOURCES OF ERROR

There are many other sources of errors which affect GNSS signals. Outlined below are some of the other major sources of error.

The troposphere can result in range errors up to 2.6 m when the satellite is at the zenith

[Langley, 1998]. As satellites approach the horizon this error can grow to 20 m [Wells et al., 1986]. However, since the troposphere is not a dispersive medium we cannot reduce its effect by using linear combinations of carrier phase observables. The best option to cope with the troposphere is to employ methods such as choosing an elevation angle cutoff of 15 degrees and modeling the troposphere.

Clock bias is another source of error that must be dealt with for precise positioning. This error results from differences in the receiver clocks and the satellite clocks. It is possible to mitigate clock bias by using a second order polynomial to approximate any drift or it can be removed by double differencing between receivers [Wells et al., 1986].

Orbit errors arising from incorrectly predicting the position of the satellite in space can be on the magnitude of three metres Root Mean Square (RMS) [Misra and Enge 2001]. These errors can be reduced if the solution is not needed in real time by using the precise ephemeris produced by the International GNSS Service (IGS). These come in three formats with the most accurate having a latency of approximately 13 days with a precision of 3 cm [IGS, 2005].

2.2 AMBIGUITY RESOLUTION

In order to achieve centimetre level accuracy it is necessary to use carrier phase signals for positioning. The benefit of carrier phase positioning is that the measurements are very precise compared to the code measurements. A difficulty arises due to an ambiguity in the phase measurement. A receiver can only tell what part of a cycle it is at. It cannot say how many cycles are between the receiver and the satellite. Each time a receiver is turned on, or if satellite lock is lost, the receiver must resolve this ambiguity or correct for the cycle slip.

There are a number of methods for solving for the ambiguity present in the carrier phase observation equation. We will not go into great detail here since our analysis at the

current time will remain in the measurement domain. However, the role that linear combinations play in improving the accuracy and reliability of ambiguity resolution methods is very significant. Currently the best known methods suggested for triple frequency ambiguity resolution are the Least Squares Ambiguity Decorrelation Adjustment (LAMBDA) and the Cascading Integer Resolution (CIR) / Triple Carrier Ambiguity Resolution (TCAR). The CIR and TCAR approaches are actually the same method except for different GNSS. For more information on these methods and techniques the reader is referred to Teunnisen (1995), Jung (1999) and Vollath et al. (1998).This completes the background to satellite positioning. Next we will begin our look at linear combinations of carrier phase observations.

3.0 LINEAR COMBINATIONS OF CARRIER PHASE OBSERVATIONS

We can now begin the search for the optimal linear combinations. To do this, we will begin by deriving the multi-frequency combinations characteristics, then breakdown how to find the optimal combination for each case, and then select the combinations which have the most desirable characteristics.

3.*1 DERIVATION OF TRIPLE-FREQUENCY LINEAR COMBINATION CHARACTERISTICS*

The derivation of the triple-frequency carrier phase combinations follows Collins [1999] and Cocard et al. [2008]. For the derivation, GPS frequency naming conventions are used but it similarly applies to Galileo by substituting the proper frequency names.

Similar to Cocard et al. [2008] we only consider the simplified version of the carrier phase observations where [m] represents units of metres:

$$L_n[m] = \rho + \lambda_n N_n + I_n \,, \tag{3.1}$$

where ρ represents the geometric range and contains clock and troposphere terms, λ_n is the wavelength, N_n is the ambiguity and I is the ionospheric propagation delay on the L1, L2 and L5 carrier frequencies. The delay is added in this case because the individual components are defined as being negative. A linear combination of the three carrier phase measurements can be formed in the following manner:

$$LC[m] = \alpha L1 + \beta L2 + \gamma L5 \,, \tag{3.2}$$

where α, β, and γ are coefficients. This can be expanded to be:

$$LC[m] = \rho(\alpha + \beta + \gamma) + \alpha\lambda_{L1} N_{L1} + \beta\lambda_{L2} N_{L2} + \gamma\lambda_{L5} N_{L5} + \alpha I_{L1} + \beta I_{L2} + \gamma I_{L5} \,. \tag{3.3}$$

In order for the combination to be useful for ambiguity resolution we want to constrain the resulting ambiguity to be an integer. By constraining the geometric portion to remain unchanged we can get the expression for the ambiguity:

$$N = \frac{(\alpha\lambda_{L1}N_{L1})}{\lambda} + \frac{(\beta\lambda_{L2}N_{L2})}{\lambda} + \frac{(\gamma\lambda_{L5}N_{L5})}{\lambda}. \tag{3.4}$$

Following Collins [1999], in order for N to be an integer we can define the coefficients i, j and k to be integers:

$$i = \frac{(\alpha\lambda_{L1})}{\lambda}, j = \frac{(\beta\lambda_{L2})}{\lambda}, k = \frac{(\gamma\lambda_{L5})}{\lambda}. \tag{3.5}$$

Then by rearranging the equations in terms of i, j and k we get:

$$\alpha = \frac{(i\lambda)}{\lambda_{L1}}, \beta = \frac{(j\lambda)}{\lambda_{L2}}, \gamma = \frac{(k\lambda)}{\lambda_{L5}}. \tag{3.6}$$

The wavelength for the new linear combination can be formed from equation α+β+γ=1, which is the geometric constraint, to yield:

$$\lambda = \frac{(\lambda_{L1}\lambda_{L2}\lambda_{L5})}{(i\lambda_{L2}\lambda_{L5} + j\lambda_{L1}\lambda_{L5} + k\lambda_{L1}\lambda_{L2})}. \tag{3.7}$$

The frequency can then be formed from the above equation:

$$f = if_{L1} + jf_{L2} + kf_{L5}. \tag{3.8}$$

To get the linear combinations parameterized in units of cycles we can divide each frequency by its wavelength and combine them to get:

$$\Phi_{i,j,k}[cy] = \frac{\rho}{\lambda} + iN_{L1} + jN_{L2} + kN_{L5} - \frac{I_{L1}}{\lambda_{L1}} - \frac{I_{L2}}{\lambda_{L2}} - \frac{I_{L5}}{\lambda_{L5}}. \tag{3.9}$$

3.2 OBSERVATION NOISE

To derive the noise of the observation we use the law of error propagation. Therefore,

the observation noise in cycles is:

$$\sigma_{\Phi_{i,j,k}}[cy] = \sqrt{i^2\sigma^2{}_{\Phi_{L1}} + j^2\sigma^2{}_{\Phi_{L2}} + k^2\sigma^2{}_{\Phi_{L5}}}\ , \tag{3.10}$$

and in meters:

$$\sigma_{\Phi_{i,j,k}}[m] = \sqrt{\alpha^2\sigma^2{}_{\Phi_{L1}} + \beta^2\sigma^2{}_{\Phi_{L2}} + \gamma^2\sigma^2{}_{\Phi_{L5}}}\ . \tag{3.11}$$

For the purpose of this report the values for the standard deviations of the carrier phase observations were obtained by following the rule of thumb described in Misra and Pratap [2001], to be 1% of the wavelength. Also the correlation between frequencies was assumed to be zero.

3.3 MULTIPATH

To see the effect of multipath on the linear combination we will look at the worst case scenario. Hoffman-Wellenhof et al. [2001] shows that the worst case scenario for errors due to multipath is ¼ of the total wavelength. Since multipath is not a random error but a systematic error we have, in cycles:

$$mp_{\Phi_{i,j,k}}[cy] = i\ \ mp_{\Phi_{L1}} + j\ \ mp_{\Phi_{L1}} + k\ \ mp_{\Phi_{L5}}\ , \tag{3.12}$$

and in meters:

$$mp_{\Phi_{i,j,k}}[m] = \alpha\ \ mp_{\Phi_{L1}} + \beta\ \ mp_{\Phi_{L1}} + \gamma\ \ mp_{\Phi_{L5}}\ . \tag{3.13}$$

Now we will look at how we form the three types of combinations listed earlier, the wide-lane, ionosphere reduced, noise reduced as well as an optimal combination. We will also discuss their characteristics and discuss combinations which are of interest to us for use in satellite positioning.

3.4 WIDE-LANE CRITERIUM

For this paper we define a wide-lane as a combination which has a wavelength greater than that of L5 frequency for GPS and a wavelength greater than the E5a frequency for Galileo. This can be stated mathematically by:

For all triplets (i,j,k) for which

$$\frac{\lambda_{\mathrm{L1}}\lambda_{\mathrm{L2}}}{i\lambda_{\mathrm{L2}}\lambda_{\mathrm{L5}} + j\lambda_{\mathrm{L1}}\lambda_{\mathrm{L5}} + k\lambda_{\mathrm{L1}}\lambda_{\mathrm{L2}}} > 1, \text{ there exists } \lambda > \lambda_{L5} \tag{3.14}$$

where λ_{L5} is the wavelength of L5 or E5a. By rearranging this inequality and using the identities $r = \frac{f_1}{f_5}$ and $t = \frac{f_2}{f_5}$ we arrive at:

$$1 - ir - jt > k > -ir - jt\,. \tag{3.15}$$

Since the range of the inequality is one, there can only be one value of k for any combination of *i* and *j*. Therefore we have:

$$k = ceil(-ir - jt)\,. \tag{3.16}$$

By substituting this equation for *k* into equation (3.15) we arrive at the expression for the wavelength as a function of *i* and *j* to be:

$$\lambda(i, j) = \frac{\lambda_{L5}}{ir + jt + ceil(-ir - jt)}\,. \tag{3.17}$$

We can now investigate the cyclic relationship present in this equation similar to what Collins [1999] performed for dual-frequency GPS and Henkel and Gunther [2007] did for Galileo. If we define the period *P* and *V* for *i* and *j* respectively and substitute into equation (3.17) we get

$$\lambda(i + P, j + V) = \frac{\lambda_5}{(i + P)r + (j + V)t + ceil(-(i + P)r - (j + V)t)}\,. \tag{3.18}$$

If we then set $\lambda(i, j) = \lambda(i + P, j + V)$:

$$ir + jt + ceil(-ir - jt) = (i + P)r + (j + V)t + ceil(-(i + P)r - (j + V)t). \quad (3.19)$$

The only way for this equality to be true is if *rP* and *tV* are integers. Therefore we can constrain *i* and *j* to be:

$$\begin{matrix} i \in [1,\ 115] \\ j \in [1,\ 23] \end{matrix}. \quad (3.20)$$

Since we want to minimize the noise of the wide-lanes we should minimize the absolute values of *i* and *j* to be:

$$\begin{matrix} i \in [-57,\ \ 57] \\ j \in [-11,\ \ 11] \end{matrix}. \quad (3.21)$$

Figure 3.1shows all possible wide-lane combinations for GPS as a function of i and j. Henkel and Gunther [2007] creates a similar plot for Galileo therefore we will not reproduce it here.

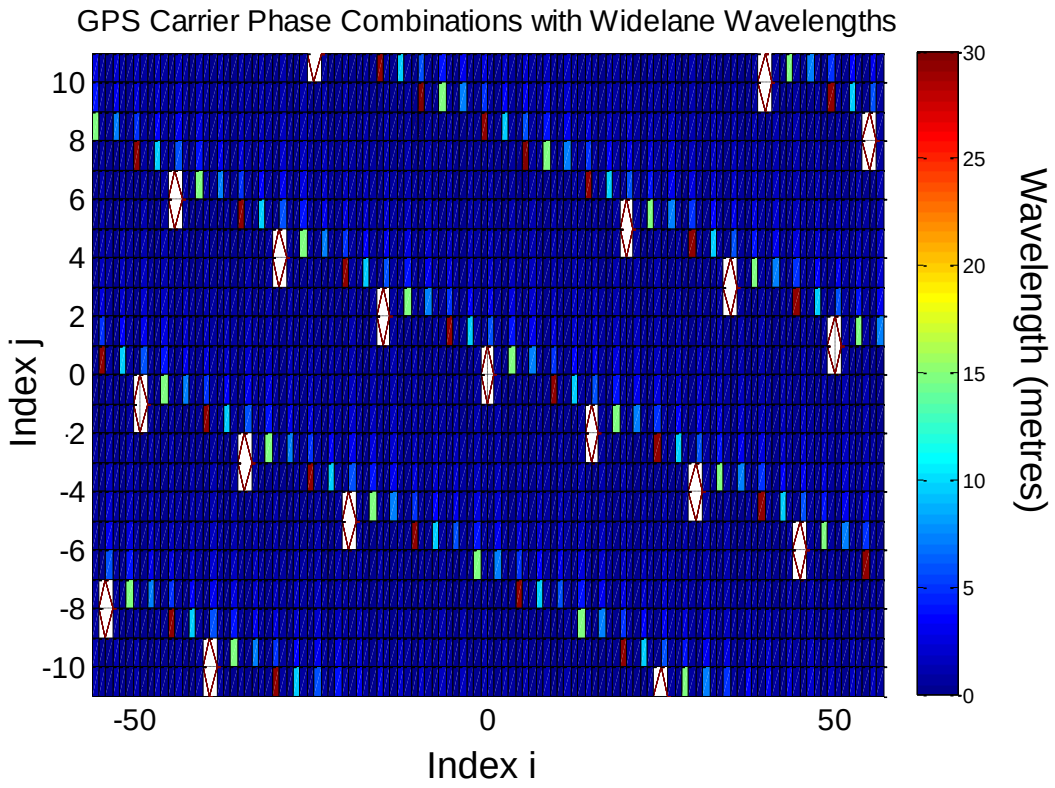

Figure 3.1 All possible wide-lane combinations as a function of i and j for GPS.

The total number of wide-lanes that can be formed by three frequencies is much greater than the number formed by just two frequencies. Even by constraining the coefficients as we have done it is still necessary to further refine the search before we can analyze the optimal wide-lanes.

To further refine the search for optimal wide-lanes, we can select combinations with other desirable properties. Table 3.1 shows the optimal wide-lane combinations for GPS. The properties shown in the table include the wavelength (λ), amplification of receiver noise (noise), first order ionospheric delay I^{1st}, multipath (mp) in units of both cycles and metres and the wavelength to noise ratio (λ /noise). In addition to this the values of the three coefficients (i, j, k) are shown. The first column (LC) uses a two letter code to describe the interesting combinations.

Table 3.1 Optimal wide-lane combinations for GPS.

						Amplification (cycles)			Amplification (metres)		
LC	i	j	k	λ(m)	λ/noise	noise	I^{1st}	mp	noise	I^{1st}	mp
	0	-1	2	0.266	0.086	2.214	1.395	0.750	3.077	1.953	4.20
ML	1	0	-1	0.751	0.136	1.407	-0.339	0.500	5.536	-1.339	7.89
WL	1	-1	0	0.862	0.136	1.407	-0.283	0.500	6.355	-1.283	9.05
	1	-2	1	1.011	0.079	2.429	-0.228	1.000	12.834	-1.208	21.24
	1	-5	4	2.093	0.030	6.418	-0.060	2.500	70.148	-0.662	110.00
HR	1	-6	5	3.256	0.025	7.797	-0.004	3.000	132.557	-0.074	205.33
	3	1	-5	4.187	0.033	5.872	-2.412	2.250	128.479	-53.071	198.00
EW	0	1	-1	5.861	0.137	1.400	-0.056	0.500	42.836	-1.719	61.60
HR	1	-7	6	7.326	0.021	9.182	0.051	3.500	351.232	1.981	539.0
	-3	1	3	9.768	0.044	4.336	2.301	1.750	221.733	118.104	359.33
HR	3	0	-4	14.653	0.038	4.968	-2.357	1.750	380.719	-181.452	539.0
HR	4	-8	3	29.305	0.020	9.357	-2.249	3.750	1433.87	-346.388	2310.0

These combinations were chosen because they either have an extremely large wavelength or minimize the error sources present while maintaining the wide-lane status. This is important because the noise and ionospheric delay amplification can also affect the chances of successful ambiguity resolution. The most common wide-lanes shown above are the extra wide-lane (EW), wide-lane (WL) and middle-lane (ML) with wavelengths of approximately 5.86 m, 0.75 m and 0.86 m respectively. Those combinations marked HR, have appeared in other literatures (i.e. Han, 1999). Also of note is the combinations [1,-5,4] which reduces the ionospheric delay, has a reasonable noise value in cycles and has a wavelength of over 2 m. However one drawback to this combination is that the noise amplification in metres is very high and could degrade the precision of the solution. Table 3.2 shows the optimal wide-lane combinations for Galileo.

Table 3.2 Optimal wide-lane combinations for Galileo

						Amplification (cycles)			Amplification (Metres)		
LC	i	j	k	λ(m)	λ/noise	Noise	I^{1st}	mp	Noise	I^{1st}	Mp
	0	2	-1	0.262	0.085	2.214	1.373	0.750	3.074	1.888	4.125
	-1	1	1	0.371	0.110	1.721	1.644	0.750	3.376	3.205	5.848
ML	1	-1	0	0.751	0.135	1.407	-0.339	0.500	5.584	-1.339	7.897
WL	1	0	-1	0.814	0.135	1.407	-0.305	0.500	6.049	-1.305	8.556
	-3	0	4	2.931	0.038	4.968	2.220	1.750	76.989	34.193	107.800
	1	9	-10	3.256	0.014	13.357	0.001	5.000	230.797	0.023	342.222
	-3	1	3	4.186	0.044	4.336	2.254	1.750	95.885	49.596	154.000
	3	-5	1	5.861	0.032	5.872	-2.391	2.250	182.195	-73.629	277.200
EW	0	-1	1	9.768	0.135	1.400	-0.034	0.500	72.583	-1.748	102.667
	3	-4	0	14.653	0.038	4.968	-2.357	1.750	384.965	-181.452	539.000
	-3	3	1	29.305	0.044	4.336	2.322	1.750	671.217	357.661	1078.000

The difference in base frequencies for Galileo results in slightly different combinations than were chosen for GPS. Again we outline the three basic middle-lane, wide-lane and extra wide-lane combinations. The EW for Galileo is 1.7 times larger than that for GPS. Additionally, we can note that the maximum wavelength for both systems is 29.31 metres. For Galileo however, this combination has less noise. The combination which has the largest wavelength to noise ratio is the combination [0, -1,1] and [1,-1,0] which are the EW and ML combinations. The value is comparable to the GPS WL combination.

Up to now a large wavelength has been described as being desirable although in reality it is not always beneficial. As was mentioned previously, a large wavelength makes solving the ambiguity easier but, if a mistake is made in solving the ambiguities this results in a larger error. This problem is compounded because as the wavelength increases so does the amplification of the noise making an incorrect solution more likely. Additionally, depending on which type of ambiguity resolution strategy is being employed it may be necessary to have further consideration placed on the combination to ensure that it is compatible with other

combinations [Cocard et al., 2008].

3.5 IONOSPHERIC DELAY REDUCED COMBINATIONS

The next type of linear combinations to be considered are those that reduce the ionospheric delay. In order to analyze the effects of the linear combinations on the higher order effects of the ionospheric refraction it is first necessary to write the ionospheric delay on each frequency in terms of the delay experienced by the L1 frequency. From equation (3.3) we have the ionospheric delay for a linear combination in meters to be:

$$I_{LC} = -\alpha I_{L1} - \beta I_{L2} - \gamma I_{L5}. \tag{3.22}$$

This can be expanded to:

$$I_{LC} = -\alpha\left[\frac{Q}{f_1^2} + \frac{S}{2f_1^3} + \frac{R}{3f_1^4}\right] - \beta\left[\frac{Q}{f_2^2} + \frac{S}{2f_2^3} + \frac{R}{3f_2^4}\right] - \gamma\left[\frac{Q}{f_5^2} + \frac{S}{2f_5^3} + \frac{R}{3f_5^4}\right]. \tag{3.23}$$

We can then relate the expressions for each order terms with respect to the delay experienced by just the L1 term as:

$$I_{LC}^{1st}[m] = -I_{L1}^{1st}\left(\alpha + \beta\frac{f_1^2}{f_2^2} + \gamma\frac{f_1^2}{f_5^2}\right), \tag{3.24}$$

$$I_{LC}^{1st}[cy] = -\frac{I_{L1}^{1st}}{\lambda_{L1}}\left(i + j\frac{f_1}{f_2} + k\frac{f_1}{f_5}\right), \tag{3.25}$$

$$I_{LC}^{2nd}[m] = -I_{L1}^{2nd}\left(\alpha + \beta\frac{f_1^3}{f_2^3} + \gamma\frac{f_1^3}{f_5^3}\right), \tag{3.26}$$

$$I_{LC}^{2nd}[cy] = -\frac{I_{L1}^{2nd}}{\lambda_{L1}}\left(i + j\frac{f_1^2}{f_2^2} + k\frac{f_1^2}{f_5^2}\right), \tag{3.27}$$

$$I_{LC}^{3rd}[m] = -I_{L1}^{3rd}\left(\alpha + \beta\frac{f_1^4}{f_2^4} + \gamma\frac{f_1^4}{f_5^4}\right), \tag{3.28}$$

$$I_{LC}^{3rd}[cy] = -\frac{I_{L1}^{3rd}}{\lambda_{L1}}\left(i + j\frac{{f_1}^3}{{f_2}^3} + k\frac{{f_1}^3}{{f_5}^3}\right), \tag{3.29}$$

with $I_{L1}^{1st} = \frac{Q}{{f_1}^2}$, $I_{L1}^{2nd} = \frac{S}{2{f_1}^3}$, $I_{L1}^{3rd} = \frac{R}{3{f_1}^4}$.

The first order term of the ionospheric delay is by far the largest. Therefore when it comes to minimizing the ionospheric delay we want combinations which satisfy:

in metres: $\left|\alpha + \beta\frac{{f_1}^2}{{f_2}^2} + \gamma\frac{{f_1}^2}{{f_5}^2}\right| < 1$ and in cycles: $\left|i + j\frac{f_1}{f_2} + k\frac{f_1}{f_5}\right| < 1$

The simplest method to find all those combinations that satisfy this inequality is to create a loop to run through the triplet of coefficients for *i*, *j* and *k*. This leaves an enormous number of possibilities. To further refine the search we can narrow down the possibilities based on the other characteristics such as wavelength and noise amplification factors. If we perform this search for all possible combinations for GPS we arrive at Table 3.3 containing the optimal ionosphere reduced combinations. The table outlines the theoretical characteristics for each selected combination including the wavelength (λ), noise amplification (noise) and higher order ionospheric delay amplification I^{1st}, I^{2nd} and I^{3rd} in units of metres and cycles. The first column marked LC gives a two letter code to identify combinations which are of special interest to us.

Table 3.3 Optimal ionosphere reduced combinations for GPS

					Amplification (Cycles)				Amplification (Metres)			
LC	i	j	k	λ(m)	noise	I^{1st}	I^{2nd}	I^{3rd}	noise	I^{1st}	I^{2nd}	I^{3rd}
IF	0	24	-23	0.125	32.91	0.0000	-1.719	-4.507	21.42	0.0000	-1.126	-2.953
N1	1	-6	5	3.256	7.80	-0.0043	0.085	0.326	132.56	-0.0744	1.449	5.572
	3	6	-8	0.112	10.34	-0.0130	-1.464	-3.530	6.04	-0.0077	-0.861	-2.075
	4	0	-3	0.108	4.98	-0.0174	-1.380	-3.204	2.82	-0.0099	-0.784	-1.821
	8	-1	-5	0.055	9.46	0.0210	-2.613	-6.121	2.71	0.0060	-0.749	-1.755
	12	-1	-8	0.036	14.41	0.0036	-3.993	-9.325	2.74	0.0007	-0.761	-1.777
N2	13	-7	-3	0.036	15.03	-0.0007	-3.908	-8.999	2.83	-0.0001	-0.737	-1.696
	13	41	-49	0.023	64.57	-0.0007	-7.346	-18.013	7.68	-0.0001	-0.879	-2.155
IF	77	-60	0	0.006	97.25	0.0000	-21.817	-49.815	3.21	0.0000	-0.721	-1.647
IF	154	0	-115	0.003	191.51	0.0000	-52.226	-122.1	2.80	0.0000	-0.767	-1.793

Those combinations marked IF or ionosphere free eliminate the ionospheric delay. For a more extensive list of IF combinations consult Han [1999]. These were omitted in this study due to their high noise amplification.

It is not always necessary or advantageous to completely eliminate the ionospheric delay. If we choose combinations that will significantly reduce the delay we may be able to choose combinations that are less susceptible to noise and multipath effects or have a larger wavelength. Keeping this in mind two notable combinations are N1 and N2. N1 has the advantage that it significantly reduces the first order ionospheric delay and is a widelane. The downside is that it significantly increases noise as well as the higher order ionospheric delays. N2 also greatly reduces the effect of the first order ionospheric delay and has a low noise and multipath amplification. The wavelength is also much larger than the IF combinations.

Table 3.4 shows the ionosphere reduced combinations for Galileo. Again the ionosphere free combinations are marked IF. The remaining combinations are chosen in a similar manner as in the previous table. Some noteworthy combinations are W1 that has a wavelength of 3.256 m while at the same time almost eliminating the effect of the ionosphere.

Table 3.4 Optimal ionosphere reduced combinations for Galileo

					Amplification (Cycles)				Amplficiation (Metres)			
LC	i	j	k	λ(m)	Noise	I1	I2	I3	Noise	I1	I2	I3
IF	0	-115	118	0.042	163.12	0.0000	-5.243	-13.864	36.29	0.0000	-1.155	-3.054
	1	9	-10	3.256	13.36	0.0013	0.107	0.384	230.80	0.0227	1.830	6.571
	4	-2	-1	0.109	4.57	0.0167	-1.290	-3.026	2.63	0.0096	-0.741	-1.739
	4	-3	0	0.108	4.98	-0.0174	-1.380	-3.204	2.84	-0.0099	-0.784	-1.821
	8	-5	-1	0.054	9.46	-0.0007	-2.670	-6.230	2.71	-0.0002	-0.763	-1.780
	9	4	-11	0.053	14.67	0.0006	-2.563	-5.846	4.15	0.0002	-0.720	-1.643
	26	3	-23	0.018	34.69	0.0004	-7.795	-17.922	3.28	0.0000	-0.734	-1.688
	42	-7	-25	0.011	49.24	-0.0010	-13.134	-30.382	2.80	-0.0001	-0.746	-1.725
	43	2	-35	0.011	55.26	0.0003	-13.027	-29.998	3.14	0.0000	-0.737	-1.697
IF	154	-115	0	0.003	191.51	0.0000	-52.226	-122.164	2.82	0.0000	-0.767	-1.793
IF	0	-115	118	0.042	163.12	0.0000	-5.243	-13.864	36.29	0.0000	-1.155	-3.054

One issue with this combination is the high noise amplification which is the highest of any combinations present in the table. In this table we also see a triple frequency ionosphere free (IF) combination [26, 3, -23]. This is of interest because the noise for both cycles is much less than the other IF combinations and the wavelength is larger.

As is shown from the tables above in general as the effect of the ionosphere is mitigated the resultant noise goes up and the wavelength goes down. This makes choosing the optimal combination difficult. Next we will look at combinations which reduce the noise of the combinations.

3.6 NOISE REDUCTION COMBINATIONS

We now move onto the noise reduction combinations. Equation (3.10) shows that when parameterized in units of cycles, linear combinations which meet the requirement that the coefficients *i, j, k* are integers, will always increase the overall noise. However, in units of metres it is possible to reduce the noise with respect to L1 or E1. To do this we must satisfy the following inequality:

$$\sigma_{\Phi_{i,j,k}}[m] = \sqrt{\alpha^2\sigma^2_{\Phi_{L1}} + \beta^2\sigma^2_{\Phi_{L2}} + \gamma^2\sigma^2_{\Phi_{L5}}} < 1. \quad (3.30)$$

Table 3.5 and 3.6 show some noise reduction combinations for GPS and Galileo which have a wavelength greater than 5 cm.

Table 3.5 Optimal noise reduction combinations for GPS

					Amplification (Cycles)					Amplification (Metres)				
LC	i	j	k	λ(m)	Noise	mp	I^{1st}	I^{2nd}	I^{3rd}	Noise	mp	I^{1st}	I^{2nd}	I^{3rd}
	1	1	0	0.107	1.41	0.500	2.28	2.65	3.11	0.789	1.124	1.28	1.49	1.75
	1	2	0	0.074	2.22	0.750	3.57	4.29	5.23	0.863	1.173	1.39	1.68	2.04
	2	1	0	0.068	2.23	0.750	3.28	3.65	4.11	0.802	1.079	1.18	1.31	1.48
NL1	0	1	1	0.125	1.40	0.500	2.62	3.44	4.52	0.911	1.311	1.72	2.25	2.96
	1	0	1	0.109	1.41	0.500	2.34	2.79	3.40	0.803	1.145	1.34	1.60	1.95
NL	1	1	1	0.075	1.72	0.750	3.62	4.44	5.52	0.678	1.188	1.43	1.76	2.18
	1	2	1	0.058	2.43	1.000	4.91	6.09	7.63	0.731	1.210	1.48	1.84	2.31
	2	0	1	0.069	2.23	0.750	3.34	3.79	4.40	0.811	1.092	1.22	1.38	1.60
	1	1	2	0.058	2.43	1.000	4.96	6.23	7.92	0.738	1.222	1.52	1.90	2.42

Table 3.5 shows that the optimal noise reduction combination is NL because it has the largest reduction factor of all the possible combinations. NL1 is noteworthy for having the largest wavelength of the group while at the same time reducing the receiver noise present. The ionospheric delay for the entire noise reduction set is slightly amplified although it is still fairly small. Table 3.6 shows the same combinations for Galileo.

Table 3.6 Optimal noise reduction combinations for Galileo

					Amplification (Cycles)					Amplification (Metres)				
LC	i	j	k	λ(m)	Noise	mp	I^{1st}	I^{2nd}	I^{3rd}	Noise	mp	I^{1st}	I^{2nd}	I^{3rd}
	2	1	1	0.054	2.44	1.000	4.64	5.50	6.62	0.70	1.139	1.32	1.56	1.89
	1	1	2	0.058	2.43	1.000	4.95	6.20	7.85	0.75	1.220	1.51	1.89	2.39
	1	2	1	0.058	2.43	1.000	4.98	6.29	8.03	0.75	1.227	1.53	1.93	2.46
	2	0	1	0.069	2.23	0.750	3.31	3.70	4.22	0.81	1.085	1.19	1.34	1.53
	1	0	2	0.075	2.22	0.750	3.61	4.41	5.45	0.88	1.185	1.43	1.74	2.15
NL	1	1	1	0.076	1.72	0.750	3.64	4.50	5.62	0.69	1.194	1.45	1.79	2.24
	1	0	1	0.108	1.41	0.500	2.31	2.70	3.22	0.80	1.132	1.31	1.53	1.82
	1	1	0	0.109	1.41	0.500	2.34	2.79	3.40	0.81	1.145	1.34	1.60	1.95
NL1	0	1	1	0.126	1.40	0.500	2.64	3.50	4.62	0.93	1.322	1.75	2.31	3.06

The combination which minimizes noise for Galileo is [1,1,1] which we have denoted as NL. This combination does a slightly worse job of mitigating noise than its equivalent combination for GPS. Additionally, we have the combination NL1 which is the largest wavelength and is slightly larger than the equivalent combination for GPS.

As with the ionosphere reducing combinations we again see the same pattern where by reducing one error amplifies another. For all noise reducing combinations we see that the ionospheric delay is increased. Additionally, all of these combinations have a wavelength less than that of L1 and E1 which makes ambiguity resolution difficult. Further on we will discuss if the choice of the narrow lane combination is an optimal choice for precise positioning.

3.7 OPTIMAL LINEAR COMBINATION

Selecting an optimal linear combination can be a fairly arbitrary task. Depending on the conditions at a given site the linear combination that will provide the best result will vary temporally. In our case the simulated scenario involves an individual receiver with moderate to high error sources. Since there is no option for double differencing, atmospheric errors are the

main contributor to the error budget. A second concern is the precision of the observable therefore low noise amplification is desirable.

The last consideration for the optimal linear combination is choosing a reasonable wavelength so that ambiguity resolution is possible. Although the wavelength necessary for successful ambiguity resolution varies it is possible to define a range which ambiguity resolution is most likely. Other research into optimal linear combinations has typically resulted in wavelengths on the order of 0.10 metres and it has been shown that even with wavelengths of this size it is still possible to properly solve for the ambiguities (eg. Richert, [2007] and Radovanic [2002]). This is also supported by the fact that the narrow-lane combination [1,1,0] used in many dual frequency positioning schemes has a wavelength of approximately 0.10 metres and it is still possible to successfully resolve its ambiguity.

Unfortunately, orbital and tropospheric delay are geometric errors meaning that they are independent of frequency so we cannot reduce these magnitude of these errors in units of metres by using linear combinations. The two major sources of error which can be mitigated by linear combinations are the noise and the ionospheric delay. These will be the focus of choosing the optimal combinations. Figure 3.2 shows the numerical optimization problem which we are trying to solve. The grey area is the ionosphere free plane showing all combinations which completely remove the first order delay and the concentric spheres show the noise contours in metres.

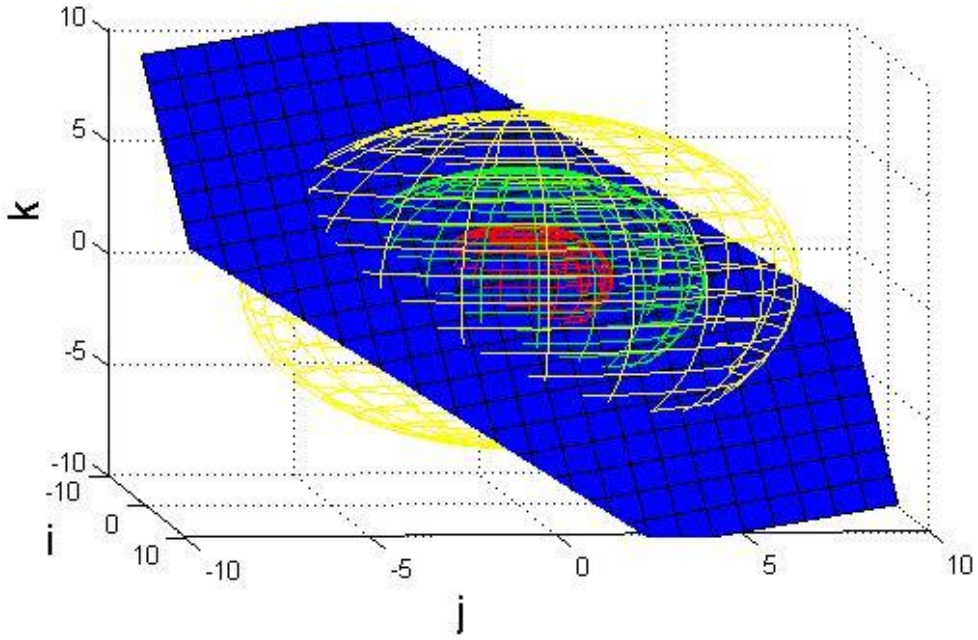

Figure 3.2 The optimization problem

From this figure we can see that an optimal combination is one that is near the ionosphere free plane and near the centre of the concentric spheres indicating a low noise amplification value. Finally we must also have a wavelength of approximately 0.10 m to allow for ambiguity resolution.

A search was made for all coefficients i, j, k $\in$ [-50, 50] since anything higher would result in noise values too high. Table 3.7 and 3.8 summarize the results of the optimization problem for GPS and Galileo.

Table 3.7 Optimal combinations for GPS

				Amplification (Cylces)					Amplification (Metres)				
i	j	k	λ(m)	Noise	mp	I^{1st}	I^{2nd}	I^{3rd}	Noise	mp	I^{1st}	I^{2nd}	I^{3rd}
4	1	-4	0.1062	5.715	2.25	-0.073	-1.53	-3.49	3.177	5.02	-0.04	-0.85	-1.95
4	0	-3	0.1081	4.982	1.75	-0.017	-1.38	-3.2	2.824	3.98	-0.01	-0.78	-1.82
4	-1	-2	0.1102	4.572	1.75	0.0384	-1.23	-2.92	2.642	4.05	0.022	-0.71	-1.69
5	-5	1	0.1028	7.105	2.75	-0.078	-1.44	-3.17	3.828	5.94	-0.04	-0.78	-1.71

Table 3.8 Optimal Combinations for Galileo

				Amplification (Cycles)					Amplification (Metres)				
i	j	k	λ(m)	Noise	mp	I^{1st}	I^{2nd}	I^{3rd}	Noise	mp	I^{1st}	I^{2nd}	I^{3rd}
4	0	-3	0.1119	4.982	1.75	0.085	-1.11	-2.67	2.939	4.11	0.050	-0.65	-1.57
4	-1	-2	0.1106	4.572	1.75	0.051	-1.20	-2.85	2.663	4.07	0.029	-0.70	-1.65
4	-2	-1	0.1093	4.572	1.75	0.017	-1.29	-3.03	2.633	4.02	0.010	-0.74	-1.74
4	-3	0	0.1081	4.982	1.75	-0.017	-1.38	-3.20	2.841	3.98	-0.010	-0.78	-1.82
4	-4	1	0.1070	5.715	2.25	-0.051	-1.47	-3.38	3.228	5.06	-0.029	-0.83	-1.90
4	-5	2	0.1058	6.665	2.75	-0.085	-1.56	-3.56	3.729	6.12	-0.048	-0.87	-1.98

The results for both systems are fairly similar. All of the wavelengths are somewhat less than the L1 or E1 wavelength however they are still reasonably large being approximately equal to the narrow-lane combinations for each respective system. Secondly, the ionospheric delay is greatly reduced for all combinations. This was expected as we are not assuming the use of double differencing between two antennas over a short baseline. From this analysis the combinations which performs the best are [4, 0, 3] for GPS and [4,-2,-1] and [4, -3, 0] for Galileo. Further analysis using simulated data will be done on all of these combinations to see which ones are truly the optimal choices for future positioning scenarios.

4.0 SIMULATION

This section provides the background information for the simulated data which will be used to evaluate the triple-frequency carrier phase linear combinations. Since there is still nearly a decade before the modernized GNSS will be fully deployed this is the best option for testing the theoretical values.

First an outline of the SimGNSS II program will be given, then a description of the methodology behind creating the simulated data and finally an explanation of the option file used in the simulation.

4.1 SIMGNSS II

SimGNSS II is a software simulator program developed in C++ to simulate GNSS observations at the University of Calgary. The simulator models five types of errors: orbital error, ionospheric error, tropospheric error, multipath, and receiver noise. For an in-depth look at the error models the following literature should be consulted:

- Ionosphere Error Model: combined Spherical Harmonics (SPHA) and grid model [Luo, 2001].
- Multipath Error Model: UofC [Ray, 2000].
- Troposphere Error Model: modified Hopfield model [Luo, 2001].
- Orbital Error Model: Based on broadcast ephemeris as described in [Luo, 2001].

The program is capable of simulating both GPS and Galileo observations although for this research only GPS observations were available.

To simulate observations SimGNSS II requires an option file as input. The option file contains all of the data concerning date, time, number of users, test location, ionospheric

model, cycle slip occurrence, scale factors for errors and noise levels. The option file can be edited in any way to suit the user's requirements. An example of an option file can be seen in Appendix I.

Now that we know how the program works we can look at how we chose the different scenarios for the simulation.

4.2 METHODOLOGY

As mentioned earlier, the full deployment of modernized GPS and Galileo constellations are still quite a few years away. Simulating these observations is the optimal method for comparing the carrier phase combinations at the present time. Two scenarios were simulated to evaluate the linear combinations. The first scenario assumes that the observations are free of biases. This is similar to short baseline applications where the atmospheric errors cancel through double differencing. The second scenario has all common errors sources present. This represents a long baseline or the case of only one receiver.

To create each scenario different values are entered into the options file to simulate the conditions that are required. The documentation which comes with the program gives values to simulate moderate to high levels of each error. These are shown in Table 4.1.

Table 4.1 Scale factors to simulate moderate to high levels of error

Parameter	Scale Factor
Multipath	0
Orbital	1
Noise	0.5
Troposphere	0.2
Ionosphere	3.2
[Lachapelle et al., 2006]	

Table 4.2 shows the values in the option files. The actual option files are attached as appendix 8.0.

Table 4.2 Input values for option files for SimGNSSII program

	Simulation Type	
	Noise	Normal Conditions
System (GPS	GPS	GPS
GPS Week	1443	1443
GPS Time To Start (s)	0	0
GPS Time To End (s)	10800	10800
Satellites		
Mask Angle (deg)	5	5
Users		
Num of Users	1	1
User Initial Position		
User Initial Position Lati	45.95020910	45.95020910
User Initial Position Longi	-66.64170475	-66.64170475
User Initial Position Height	22.74	22.74
Errors		
Orbit Scale Factor	0	0
Iono Scale Factor	0	3.2
Trop Scale Factor	0	0.2
Average Temperature (deg C)	20	20
Relative Humidity	0.3	0.3
Pressure mbars	1013	1013
MultiPath Scale Factor	0	0
Receiver Noise Scale Factor	1	1
Carrier Noise SF for GPS L1	0.01	0.002
Carrier Noise SF for GPS L2	0.01	0.002
Carrier Noise SF for GPS L5	0.01	0.002
Cycle Slips	None	None

Although the time and location of the test has essentially no effect on the results, the University of New Brunswick was chosen as the location. The simulation occurred on September 2nd 2007 and lasted three hours. This allows for a variation in the levels of ionosphere and troposphere activity. A mask angle of 5 degrees and standard temperature and humidity were chosen. The choice of receiver noise level followed the typical rule of thumb of 1% of the wavelength. This level of noise is comparable to other research which utilized this software [e.g. Alves, 2001, Hein et al., 2002 and Richert, 2007]. Orbital errors were set to zero since they are independent of frequency and with the use of the final precise orbits this error would be minimal. Tropospheric effects are also independent of frequency. For this reason we chose to model its effects using UNB3m. UNB3m uses standard atmospheric look up tables and computes the total zenith delay based on receiver location, height and day of year. The zenith delay is then mapped to the elevation angle using a Neill mapping function [Leandro et al., 2006]

Since we are analyzing the results in the measurement domain it is necessary to simulate error free observations so that we can separate the errors from the carrier phase observables. By using the simulator and setting all of the error parameters to zero we can generate this error free observable set. The output from the simulation for the carrier phase measurements are in cycles. To compare the observations the first step is to apply the linear combination to both the error free set and the set containing errors. We can then subtract the error free observation set from the simulated observations leaving only the errors present.

To compare the linear combinations in units of metres one extra step is needed. After the linear combinations are applied we then need to parameterize the observations in units of metres by multiplying the carrier phase observations by the wavelength of the respective carrier phase. We can then subtract the observables and get the final results. This process is

shown in Figure 4.1.

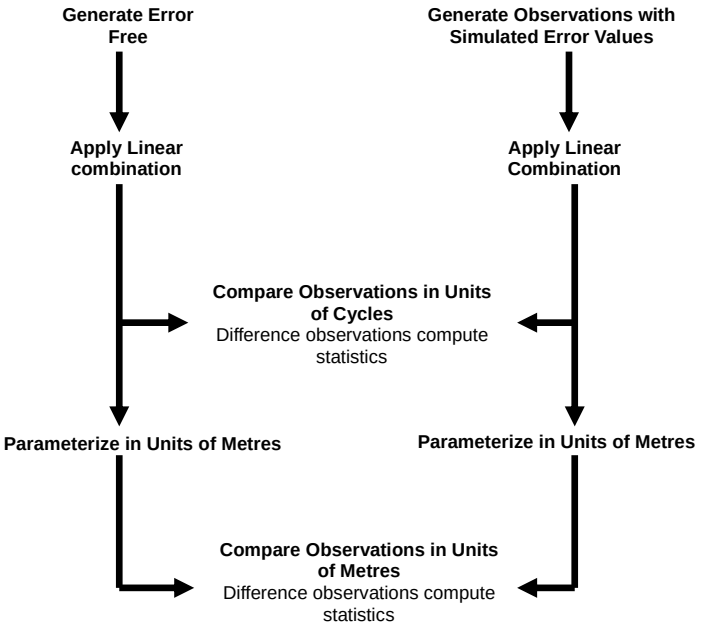

Figure 4.1 Flow chart of the analysis of linear combinations

For the analysis it is necessary to choose one satellite. Although this is a rather arbitrary task there are a number of characteristics which are more desirable. For the analysis it is necessary for the satellite to be visible for the entire test period. Additionally, since most observation sessions exclude satellites with extremely low elevation angles we want to avoid those which are below 10 or 15 degrees. At the opposite end of the spectrum it is unlikely to have a satellite to pass directly overhead so in choosing the satellite an elevation angle ranging between 15 and 85 degrees is considered reasonable.

Viewing the output of the simulation file, PRN 17 was chosen. Figure 4.2 on the following page shows the elevation angle vs. time for PRN 17. The plot shows that at no time during the observation period does the elevation angle become greater than 85 degrees or less than 55 degrees which fits the criteria laid out previously.

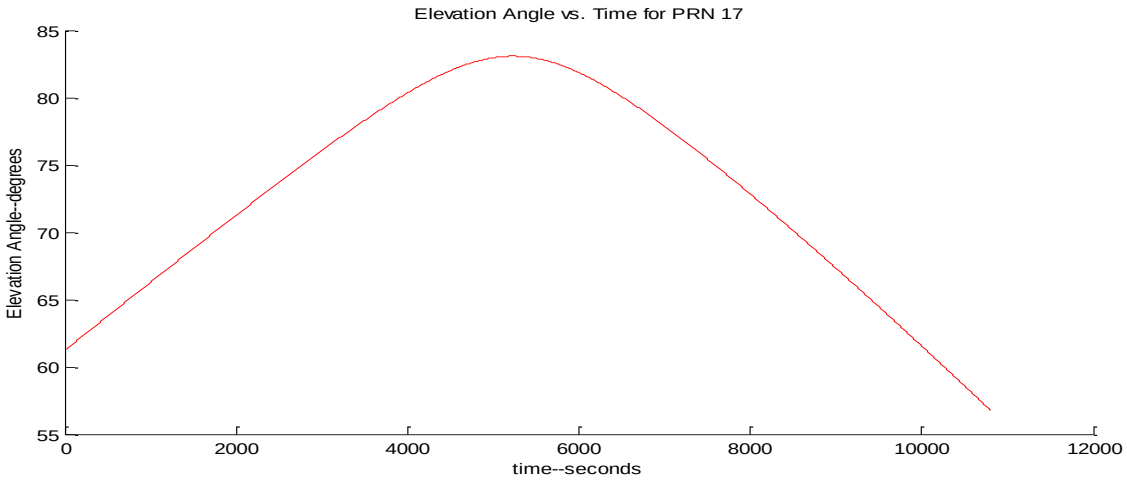

Figure 4.2 Elevation angle vs. time for PRN 7

We are now ready to analyze the results of the simulation and determine the optimal linear combinations. At the present time it is not possible to get observations for Galileo therefore only the GPS optimal combinations will be tested.

5.0 ANALYSIS OF RESULTS

In the following section the analysis of the reduced ionospheric delay, noise reduction and optimal linear combinations which were derived in the previous sections will be performed. There is no specific analysis performed for the wide-lane because this property is a factor in determining the optimal combination in order to allow for proper ambiguity resolution. Additionally, it will be shown that the narrow-lane combination may not be the optimal choice to reduce the noise of the observations.

5.1 REDUCED IONOSPHERIC DELAY COMBINATIONS

To determine the effectiveness of the linear combinations for reducing the ionospheric delay a statistical analysis is performed on the raw observations. The troposphere has been removed since it is a geometric error and is frequency independent. Figure 5.1 on the following page shows the ionospheric delay present on the three carrier frequencies in metres for the carrier phase for PRN 17 before any linear combinations have been applied. The total error ranges from 10 metres for the L1 frequency to approximately 20 metres for the L2 and L5 frequencies.

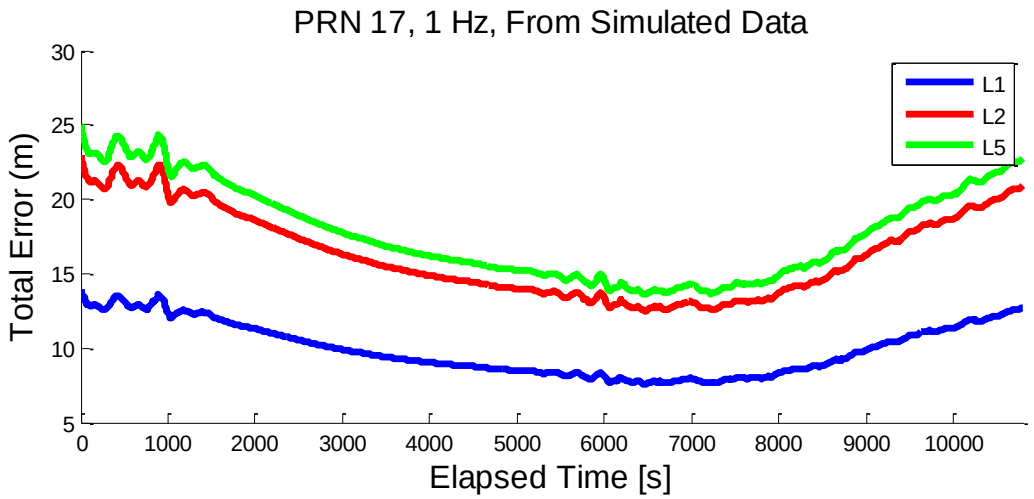

Figure 5.1 Total Error on L1, L2 and L5 Frequencies

Table 5.1 shows the results of applying the optimal linear combinations for reducing the ionospheric delay.

Table 5.1 Statistical results for linear combinations which reduce ionospheric delay on simulated observations

i	j	k	LC	Standard Deviation	Mean	Max	Min	Amp. Factor
1	0	0	L1	1.758	9.916	13.959	7.590	1.0000
0	24	-23	(IF)	0.004	0.000	0.016	-0.016	0.0000
1	-6	5		0.133	-0.738	-0.487	-1.081	-0.0744
3	6	-8		0.014	-0.076	-0.055	-0.109	-0.0077
4	0	-3		0.017	-0.098	-0.074	-0.138	-0.0099
8	-1	-5		0.011	0.060	0.084	0.045	0.0060
12	-1	-8		0.001	0.007	0.010	0.004	0.0007
13	-7	-3		0.001	-0.001	0.001	-0.004	-0.0001
13	41	-49		0.001	-0.001	0.005	-0.006	-0.0001
77	-60	0	(IF)	0.001	0.000	0.002	-0.002	0.0000
154	0	-115	(IF)	0.001	0.000	0.002	-0.002	0.0000

For the IF combinations we can see that the error has been completely removed. The standard deviations are still on the millimetres level due to the receiver noise. Additionally, the

amplification factors are very comparable to the theoretical values which verifies our models used in the derivation of the ionosphere reduced combinations. One note of caution, it was impossible to determine if the simulation software accounts for higher order ionosphere values or only for the first order error. This may make the results slightly optimistic.

Figures 5.2 shows the ionospheric delay in metres for the three ionosphere free combinations. The simulation confirms that the IF combinations completely remove the ionospheric delay.

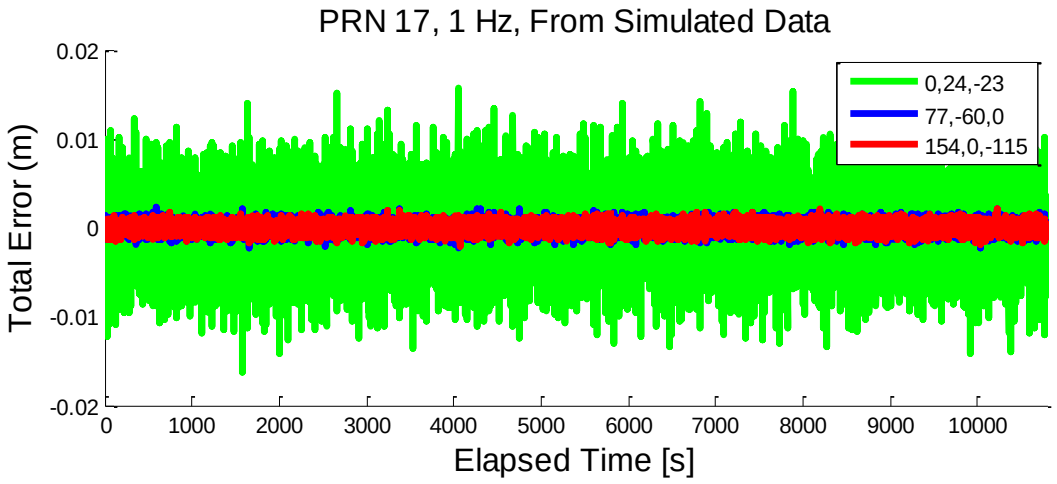

Figure 5.2 Total Error for the ionosphere free combinations

Although all three of the IF combinations remove the ionospheric delay we can see that they are not equal due to the amplification of receiver noise. The most effective combination is actually the L1/L5 combinations [154,0,-115] which has the lowest standard deviation. The L2/L5 combination performs the worst while L1/L2 is similar to the L1/L5 combination. This could be very important for applications which may take place in high noise or high multipath environments. Careful consideration based on the specific application is needed to choose the ideal combination for a given user.

Another combination of note is [13,-7,-3]. This combination is the best non-ionosphere

free combination for reducing the effect of the ionospheric delay. Figure 5.3 shows that by using the combination [13,-7,-3] we can reduce the ionospheric delay to the millimetre level. The main advantage to this combination is that the noise levels in metres are similar to the ionosphere free combinations but the wavelength is much larger than the L1/L5 or the L1/L2 combinations and a noise level much lower than the L2/L5 combination. This means that it may be more desirable to use this combination rather than the traditional ionosphere free combinations.

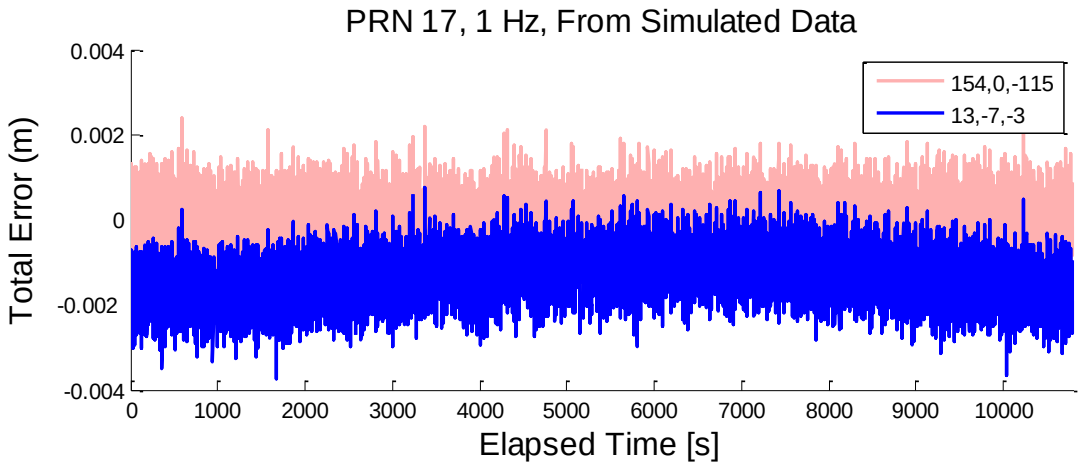

5.3 Total Error for Combination [13,-7,-3] and [154,0,-115].

5.2 NOISE REDUCTION COMBINATIONS

For the noise reduction analysis the bias free observations are used. This simulates the scenario we may see if we have a very short baseline and the distance dependent effects such as atmospheric errors cancel through double differencing. Figure 5.4 shows the noise that is present on three carrier frequencies for PRN 17. The standard deviation of the noise is on the order of 0.5 mm. Although this is low the actual noise value we are only interested to see the reduction in noise that can be achieved through the use of linear combinations.

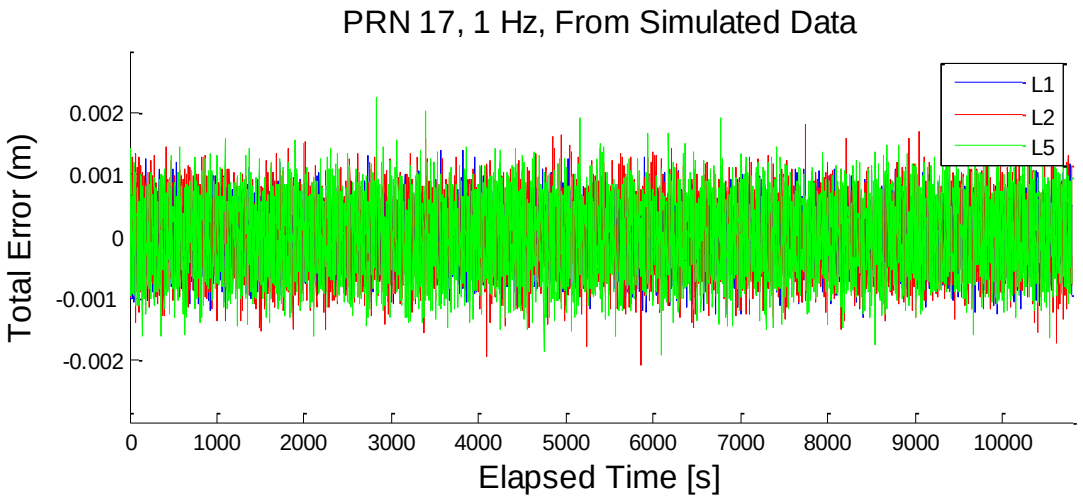

Figure 5.4 Receiver noise on the L1 L2 and L5 frequencies

Table 5.2 shows the results of applying the linear combinations. The theoretical values for the amplification factors calculated in section 3.6 match the values of the simulation very well. From Table 5.2 we can see that the optimal noise reduction combinations perform very similar for this test. The combinations [1,1,1] does perform slightly better with the lowest amplification factor.

Table 5.2 Statistical results for linear combinations which reduce noise on simulated observations

i	j	k	Standard Deviation	Mean	Max	Min	Amp. Factor
1	0	0	0.0004	0.0000	0.0016	-0.0013	1.0000
1	1	0	0.0003	0.0000	0.0010	-0.0012	0.7901
1	2	0	0.0003	0.0000	0.0011	-0.0013	0.8670
2	1	0	0.0003	0.0000	0.0012	-0.0011	0.8021
0	1	1	0.0003	0.0000	0.0012	-0.0012	0.9133
1	0	1	0.0003	0.0000	0.0015	-0.0012	0.8045
1	1	1	0.0003	0.0000	0.0012	-0.0009	0.6766
1	2	1	0.0003	0.0000	0.0010	-0.0010	0.7308
2	0	1	0.0003	0.0000	0.0013	-0.0012	0.8109
1	1	2	0.0003	0.0000	0.0013	-0.0010	0.7386

Figure 5.5 shows the improvement that can be achieved by using the triple frequency

narrow-lane combination over the L1 only observable. If the noise levels were higher the improvement would be even more visible.

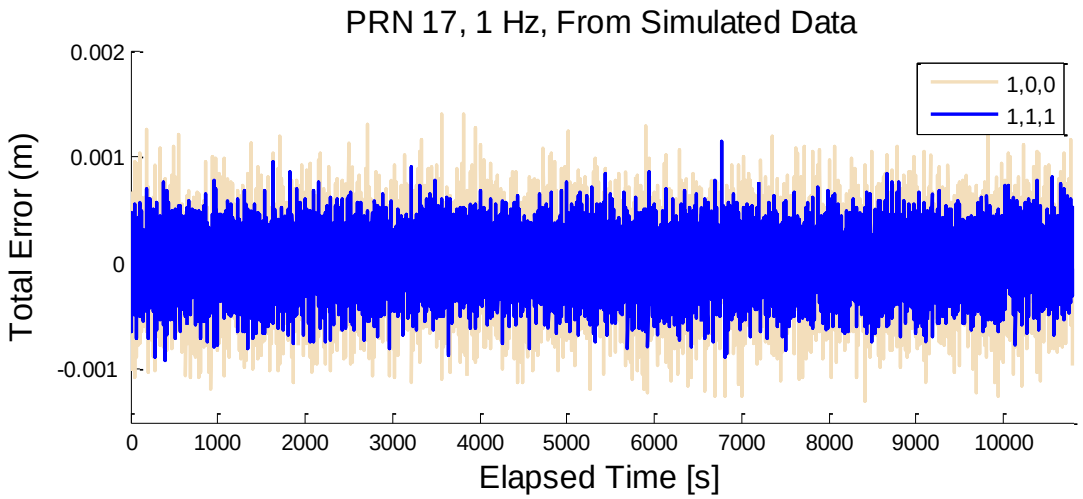

Figure 5.5 Receiver noise in metres for triple frequency NL combination and L1 observable

Figure 5.6 shows that the addition of a third frequency does not greatly improve the nose reduction capabilities compared to the L1/L2 narrow-lane. There may also be drawbacks to using the triple frequency narrow-lane which we will discuss in a moment.

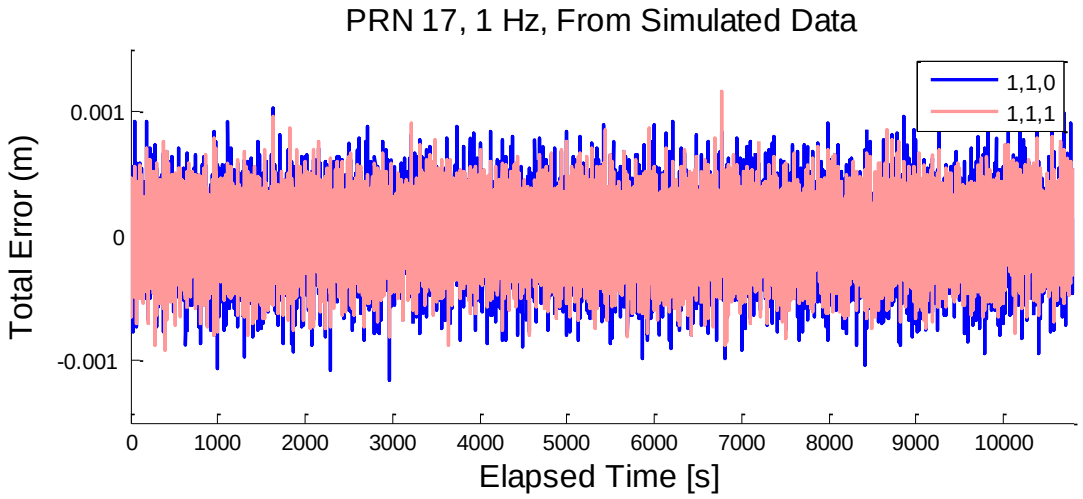

Figure 5.6 Receiver noise in metres for triple frequency and dual frequency NL

Although the above plots and statistical analysis shows that there is an improvement in

the measurement domain of precision of the carrier phase measurements, if we now consider the position domain we can mathematically show that the narrow-lane [1,1,1] may not be the optimal use of the triple frequency data. Petovello [2006] shows that by using the L1 and L2 frequencies independently it is possible to get improved precision. Additionally, it decreases the likelihood of incorrect ambiguity resolution which is caused by the wavelength of the narrow-lane combination being so small.

If we follow the least squares adjustment technique outlined in Hoffman-Wellenhof [2001] we have the linearized observation model represented in matrix-vector notation as:

$$\underline{\ell}_i = \underline{\underline{A}}_i \underline{x}_i , \tag{5.1}$$

where $\underline{\ell}_i$ is the vector of observations for frequency *i*, $\underline{A}_i$ is the design matrix consisting of direction cosines to the various satellites scaled by the carrier wavelength (i.e., $A_i=A/\lambda_i$), and $\underline{x}_i$ is the vector of unknowns. By applying the least squares principle we then have the solution for $\underline{x}_i$ to be:

$$\underline{x}_i = (\underline{A}_i^T \underline{P}_i \underline{A}_i)^{-1} \underline{A}_i^T \underline{P}_i \underline{\ell}_i , \tag{5.2}$$

where the weight matrix $\underline{P}_i$ is equal to:

$$\underline{P}_i = \frac{1}{\sigma_o^2} \underline{C}_{\ell_i}^{-1} , \tag{5.3}$$

where σ_o^2 is the apriori variance and $\underline{C}_{\ell i}$ is the covariance matrix of the observations for frequency *i*. We can then expand equation (5.2) out to become

$$\underline{x}_{L1+L2+L5} = \left(\begin{bmatrix} \frac{\underline{A}_{L1}^T}{\lambda_{L1}} & \frac{\underline{A}_{L2}^T}{\lambda_{L2}} & \frac{\underline{A}_{L5}^T}{\lambda_{L5}} \end{bmatrix} \begin{bmatrix} \underline{P}_{\ell L1} & 0 & 0 \\ 0 & \underline{P}_{\ell L2} & 0 \\ 0 & 0 & \underline{P}_{\ell L5} \end{bmatrix} \begin{bmatrix} \frac{\underline{\underline{A}}_{L1}}{\lambda_{L1}} \\ \frac{\underline{\underline{A}}_{L2}}{\lambda_{L2}} \\ \frac{\underline{\underline{A}}_{L5}}{\lambda_{L5}} \end{bmatrix} \right)^{-1} \times \begin{bmatrix} \frac{\underline{A}_{L1}^T}{\lambda_{L1}} & \frac{\underline{A}_{L2}^T}{\lambda_{L2}} & \frac{\underline{A}_{L5}^T}{\lambda_{L5}} \end{bmatrix} \begin{bmatrix} \underline{P}_{\ell L1} & 0 & 0 \\ 0 & \underline{P}_{\ell L2} & 0 \\ 0 & 0 & \underline{P}_{\ell L5} \end{bmatrix} \begin{bmatrix} \underline{\ell}_{L1} \\ \underline{\ell}_{L2} \\ \underline{\ell}_{L5} \end{bmatrix}$$

(5.4)

Then by substituting equation (5.3) into equation (5.4):

$$\underline{x}_{L1+L2+L5} = \left(\frac{\underline{A}_{L1}^T \underline{C}_{\ell\ L1}^{-1} \underline{A}_{L1}}{\sigma_o^2 \lambda_{L1}^2} + \frac{\underline{A}_{L2}^T \underline{C}_{\ell\ L2}^{-1} \underline{A}_{L2}}{\sigma_o^2 \lambda_{L2}^2} + \frac{\underline{A}_{L5}^T \underline{C}_{\ell\ L5}^{-1} \underline{A}_{L5}}{\sigma_o^2 \lambda_{L5}^2} \right)^{-1} \times \left(\frac{\underline{A}_{L1}^T \underline{C}_{\ell\ L1}^{-1} \underline{\ell}_{L1}}{\sigma_o^2 \lambda_{L1}^2} + \frac{\underline{A}_{L2}^T \underline{C}_{\ell\ L2}^{-1} \underline{\ell}_{L2}}{\sigma_o^2 \lambda_{L2}^2} + \frac{\underline{A}_{L5}^T \underline{C}_{\ell\ L5}^{-1} \underline{\ell}_{L5}}{\sigma_o^2 \lambda_{L5}^2} \right)$$

. (5.5)

Finally, the covariance of the L1+L2+L5 solution is given by the first half of equation (5.5) which can be simplified to :

$$\underline{C}_{\underline{x}_{L1+L2+L5}} = \left(\frac{\underline{A}_{L1}^T \underline{C}_{\ell\ L1}^{-1} \underline{A}_{L1}}{\sigma_o^2 \lambda_{L1}} + \frac{\underline{A}_{L2}^T \underline{C}_{\ell\ L2}^{-1} \underline{A}_{L2}}{\sigma_o^2 \lambda_{L2}} + \frac{\underline{A}_{L5}^T \underline{C}_{\ell\ L5}^{-1} \underline{A}_{L5}}{\sigma_o^2 \lambda_{L5}} \right)^{-1} = \sigma_o^2 \frac{\lambda_{L1}^2 \lambda_{L2}^2 \lambda_{L5}^2}{\lambda_{L1}^2 + \lambda_{L2}^2 + \lambda_{L5}^2} \left(\underline{A}^T \underline{C}_\ell^{-1} \underline{A} \right)^{-1}$$

.(5.6)

The development of the narrow-lane solution (NL) in the position domain can be realized in a similar manner to that of the L1+L2+L5 solution. We have:

$$\underline{x}_{NL} = \left(\frac{\underline{A}_{NL}^T}{\lambda_{NL}} \underline{P}_{\ell NL} \frac{\underline{A}_{NL}^T}{\lambda_{NL}} \right)^{-1} \times \frac{\underline{A}_{NL}^T}{\lambda_{NL}} \underline{P}_{\ell NL} \underline{\ell}_{NL} . \tag{5.7}$$

Once again the covariance of the NL solution is given by the first part of equation (5.7) and by substituting, $\underline{P}_{\ell NL} = \frac{1}{\sigma_o^2} \underline{C}_\ell^{-1}$:

$$\underline{C}_{NL} = \sigma_o^2 \left(\frac{\underline{A}_{NL}^T}{\lambda_{NL}} \underline{C}_\ell^{-1} \frac{\underline{A}_{NL}^T}{\lambda_{NL}} \right)^{-1} \tag{5.8}$$

If we then assume that the standard deviation of the three observations are equal then by error propagation we have:

$$\sigma_o^2 = \sigma_{NL}^2 = \sigma_{L1}^2 + \sigma_{L2}^2 + \sigma_{L5}^2 = 3\sigma^2 . \tag{5.9}$$

We can further develop equation (5.8) to get a solution for the covariance matrix of the

estimated parameters for the NL solution by substituting equation (3.7) for the wavelength of the NL, λ_{NL} combination where ({i, j, k} =1)

$$\underline{\underline{C}}_{\underline{\hat{x}}_{NL}} = 3\sigma^2 \frac{\lambda_{L1}^2 \lambda_{L2}^2 \lambda_{L5}^2}{(\lambda_{L1} + \lambda_{L2} + \lambda_{L5})^2} \left(\underline{\underline{A}}^T \underline{\underline{C}}_{\ell}^{-1} \underline{\underline{A}} \right)^{-1}. \tag{5.10}$$

We can now compare the covariance matrix of the estimated parameters for the NL, equation (5.10), and L1+L2+L5, equation (5.6), solutions by looking at the ratios between the two matrices. We have

$$\frac{\underline{\underline{C}}_{\underline{\hat{x}}_{L1+L2+L5}}}{\underline{\underline{C}}_{\underline{\hat{x}}_{NL}}} = \frac{1}{3\cancel{\sigma^2}} \frac{(\lambda_{L1} + \lambda_{L2} + \lambda_{L5})^2}{\cancel{\lambda_{L1}^2 \lambda_{L2}^2 \lambda_{L5}^2}} \cancel{\sigma^2} \frac{\cancel{\lambda_{L1}^2 \lambda_{L2}^2 \lambda_{L5}^2}}{\lambda_{L1}^2 + \lambda_{L2}^2 + \lambda_{L5}^2}, \tag{5.11}$$

$$\frac{\underline{\underline{C}}_{\underline{\hat{x}}_{L1+L2+L5}}}{\underline{\underline{C}}_{\underline{\hat{x}}_{NL}}} = \frac{1}{3} \frac{(\lambda_{L1} + \lambda_{L2} + \lambda_{L5})^2}{\lambda_{L1}^2 + \lambda_{L2}^2 + \lambda_{L5}^2} = 0.9851. \tag{5.12}$$

If we perform the same analysis but replace the GPS signal wavelengths with those for Galileo we see that the ratio is 0.9845. So it is shown, at least theoretically, that by using the three carrier phase observations independently there is an improvement in the precision of the solution by about 1.5%

There are a number of significant implications which arise from the narrow-lane solutions being less precise than the triple frequency solutions used independently. Petovello [2006] lists several advantages of not using the narrow-lane approach for dual frequency users. These also apply for triple frequency users. Firstly, the narrow-lane combination has a very small wavelength making ambiguity resolution more difficult. Secondly, if due to loss of lock one of the frequencies becomes unusable the narrow-lane solution will not work where as the combined solution can still produce a result. This is even more significant for the modern GNSS systems because there are three frequencies that need to be tracked. Petovello goes on to say that the only possible advantage to the narrow-lane solution is that it could reduce the

computational burden and bandwidth of the observations. However, with today's processors this would be of little to no concern unless network RTK or cellular communication is necessary.

Although the theoretical development shows that there is no advantage to using the narrowlane combination, past experience contradicts this result. Kim (2003) shows that by using the narrowlane combination there is actually an improvement in the precision of the solution. This contradiction could results from assumptions regarding the independence of the errors on each frequency. Until triple frequency data is available it will be difficult to determine which approach is optimal.

5.3 OPTIMAL LINEAR COMBINATION

Finally we arrive at the optimal combinations. These combinations are used to process the simulated observations under normal conditions which are created using moderate to high level of errors. The tropospheric error is reduced by using the UNB3m tropospheric delay model. Figure 5.7 shows the total error present on the L1, L2 and L5 frequencies for PRN 17.

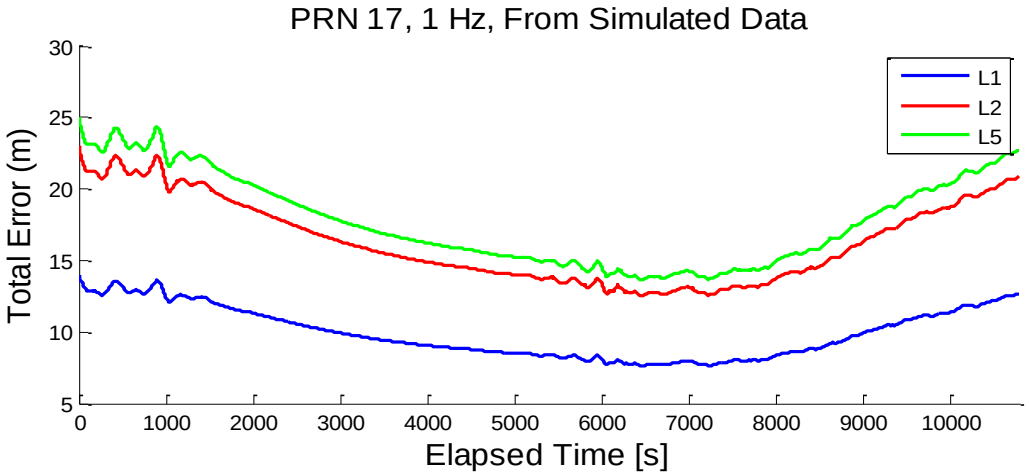

Figure 5.7 Total error on the L1,L2 and L5 frequencies in metres

The statistics for the above plot as well as those for the four optimal linear combinations are summarized in Table 5.3. As can be seen from the table there is a substantial advantage to using the optimal linear combinations.

Table 5.3 Statistical results for optimal linear combinations on simulated observations

i	j	k	Standard Deviation	Mean	Max	Min	Amp. Factor
1	0	0	1.7606	9.9382	13.9950	7.6101	1.0000
4	1	-4	0.0691	-0.3823	-0.2895	-0.5340	-0.0385
4	0	-3	0.0156	-0.0754	-0.0543	-0.1137	-0.0076
4	-1	-2	0.0424	0.2431	0.3461	0.1868	0.0245
5	-5	1	0.0710	-0.3928	-0.2968	-0.5496	-0.0395

The main component of the total error that is present on the L1 observable is the ionospheric delay, since the geometric errors have been reduced and multipath and noise terms are on the centimetre level. Since the optimal combinations all have ionosphereic amplification factors less than one it is obvious that we will see a large improvement. Figure 5.8 shows the results of applying the optimal combinations. This clearly shows that the combination [4,0,-3] performed the best with a total error nearly 20 cm less than the other combinations.

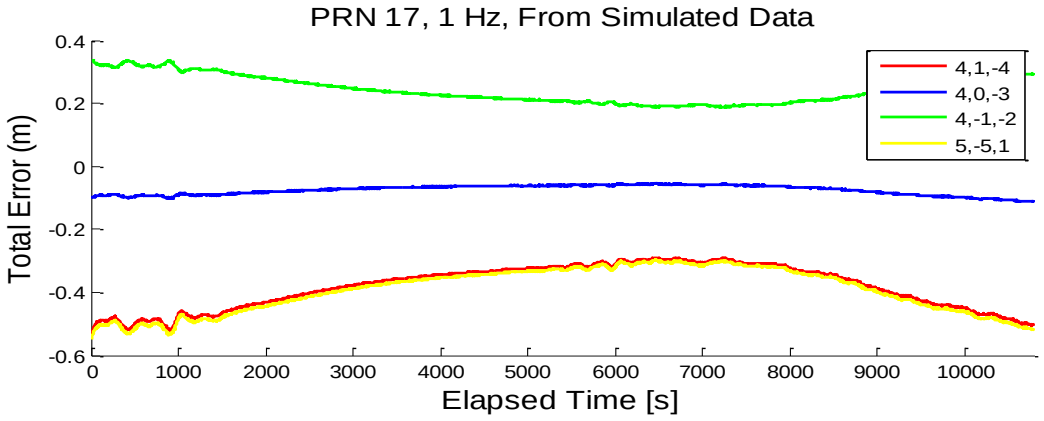

Figure 5.8 Total error for the optimal linear combinations in metres

The remaining error that can be seen in the plot mostly results from the residual atmospheric delay as well as partially from multipath and noise. Although the total error is more than that of the ionosphere free combinations that were discussed earlier, the advantage to these combinations is that the wavelength is much larger. In addition no other attempt was made to estimate or model the ionospheric delay. If a modelling scheme were implemented this would change the optimal combinations because the results would not be so heavily weighted towards reducing the ionospheric delay.

Although the results are promising there is still room for improvement. As mentioned before, the optimal combination is dependent on a large number of variables. This is one drawback of the direct approach because it does not mean that the combinations discussed above will always be ideal. This is where the inverse approach can significantly improve results by solving for the coefficients i,j,k on an epoch-by-epoch basis based on the magnitude of each error source.

From this analysis we can see that there are combinations that significantly improve the accuracy and precision of GNSS measurements. Before we can say which are truly the optimal linear combinations further study will need to be done once the systems are fully deployed.

6.0 CONCLUSIONS AND RECOMENDATIONS

The main goal of this research was to find the optimal linear combination of carrier phase observations to be used for singe receiver positioning by future GNSS. To do this it was first required to derive the characteristics of triple frequency carrier phase combinations, then search for the combinations which had the most desirable characteristics.

The two methods which have been taken in past research has been reviewed and classified as the direct approach and the inverse approach. Although both approaches have advantages and drawbacks it was suggested that the inverse approach would be more useful because of its adaptive capabilities.

The amplification factors for the higher order ionospheric terms were also derived. It was shown that in some cases the combinations reduced the first order delay but amplified the second and third order delays. This could be a concern if very precise applications where the higher order terms may make up a large portion of the error budget. For the ionosphere free combinations it was shown that the second and third order delays were amplified by 1.3 to 3.0 times. For the optimal combinations in most cases the first and second order delays were reduced but typically the third order delay was increased by a factor of 2 when parameterized in units of metres.

Finally, to evaluate these combinations simulated GNSS observations were used to analyze the performance of the combinations in the measurement domain. The simulated data complemented the theoretical results which were derived thereby verifying the models used at least with respect to the simulator. The results showed that there is a significant advantage to using optimal combinations to reduce errors present in the observation equation. However, it

was also shown that for the narrow-lane combination there may be more optimal ways to utilize the three frequencies to improve the precision of the final position.

Although the linear combinations did improve the overall accuracy, it is suggested that other methods be employed along with a linear combination in order to better account for the error sources.

Until the new GNSS are fully operational we will not be able to have a definite answer as to the optimal combinations for positioning. However, by using the simulated data we can get an advanced look into which combinations should be considered and how they can be used to improve the accuracy of satellite positioning.

There is still some further analysis which should be investigated in the future. They are as follows:

- Ambiguity resolution is not only a function of the signal wavelength. Therefore these wide-lane solutions may not always be the most optimal. Additionally, in selecting an optimal combination a fairly arbitrary wavelength was selected as a limiting factor, 10 cm. If a more theoretical approach could be used to study the effects of wavelength, and signal noise on the ambiguity resolution process it may be possible to find combinations which better account for other errors while still allowing for successful ambiguity resolution.
- This research focused on the measurement domain. In the end all that matters is how accurately and precisely we can determine a point of interest. Therefore further study into how these linear combinations affect the positioning accuracy would be desirable. So although we have determined an optimal combination in the sense that it has the most benefits in the measurement domain, further study would need to be done to see

if this translates into the optimal combination in the position domain.

- Finally, at the time of writing this report it was not possible to obtain simulated Galileo measurements. A similar analysis could be performed on those combinations which were selected and a comparison could be done to compare the two systems.
- Testing on real observations will be possible once the systems begin deployment. This will allow us to first look only at the measurement domain but eventually the position domain as more satellites become available.
- The results presented here were for a typical survey condition. Future work should involve developing the inverse approach to select an optimal combination on an epoch by epoch basis.

7.0 REFERENCES

Alves, P. (2001) . "The Effect of Galileo on Carrier Phase Ambiguity Resolution." *Proceedings of the Institute of Navigation GPS 2001*, Salt Lake City, UT, September 11 - 14, 2001, pp. 2086 - 2095.

Bassiri, S., and G. A. Hajj (1993). "High-order ionospheric effects on the global positioning system observables and means of modeling them", *Manuscripta Geodaetica*, vol. 18, p.280-289.

Cocard, M., and A. Geiger (1992). "Systematic Search for all Possible Widelanes." *Proceedings of the Sixth International Geodetic Symposium on Satellite Positioning*, Columbus Ohio March 17-20, 1992, pp. 312-318.

Cocard, M., Bourgon, S., Kamali, O., and Collins, P. (2008). "A systematic investigation of optimal carrier-phase combinations for modernized triple-frequency GPS.", *Journal of Geodesy*, Vol. 82, pp. 555-564, DOI: 10.1007/s00190-007-0201-x

Collins, P. (1999) "An Overview of Inter-frequency Carrier Phase Combinations." Unpublished paper. (Available online at: http://gauss.gge.unb.ca/papers.pdf/L1L2combinations.collins.pdf

Department of Defence and Department of Transportation (2001). "2001 Federal Radionavigation Systems." National Technical Information Service, 22161 DOT-VNTSC-RSPA-01-3.1/DOD-4650.5, Springfield, Virginia, pp. 126

ESA (2007). "How to Build up a Constellation of Navigation Satellites." [on-line] 26 June

2008, retrieved from http://www.esa.int

Fontana, R. D., W. Cheung, and T. Stansell (2001). "The Modernized L2 Civil Signal." *GPS World*, Vol.12, No.9, pp.28-33.

Han, S. and C. Rizos (1999). "The Impact of Two Additional Civilian GPS Frequencies on Ambiguity Resolution Strategies", *Propceedings of ION Annual Meeting,* Alexandria VA, January 25-27, 1999, pp. 315-321

Han, S. (1997). "Carrier phase-based long-range GPS kinematic positioning." UNISURV Report No. S49, School of Geomatics Engineering, University of New South Wales, Sydney, Australia, pp 185.

Han, S., and C. Rizos (1996). "Improving the computational efficiency of the ambiguity function algorithm." *Journal of Geodesy,* Vol. 70, No. 6, pp330-341.

Hein, G., J. Godet, J.-L. Issler, J.-C. Martin, P. Erhard, R. Lucas-Rodriguez and T. Pratt (2002) "Status of Galileo Frequency and Signal Design." *Proceedings of the Institute of Navigation GPS 2002*, Portland Oregon, September 24-27, 2002, pp 266-277

Henkel, P., and Günther, C. (2007). "Three frequency linear combinations for Galileo." *Proceedings of the 4th Workshop on Positioning, Navigation and Communication (WPNC'07), Hannover, Germany, pp.* 239-245.

Hoffman-Wellenhof, B., Lichtenegger, H. and Collins, J. (2001) *GPS: Theory and Practice.* Springer-Verlag, Berlin.

IGS (2005). "IGS PRODUCTS", International Global Navigation Satellite Systems Service,

[On-line] 21 December 2007, retrieved from: http://igscb.jpl.nasa.gov/components/prods.html

Inside GNSS (2007). "Transport Ministers Put Galileo Back on Track.", *Inside GNSS*, [on-line] 03 January 2008 retrieved from: http://www.insidegnss.com/node/419.

Inside GNSS (2008). "Faulty Booster Component May Delay IIR-M Launches; L5 Signal Ready to Go", [on-line] 26 June 2008 retrueved from : http://insidegnss.com

Jung, J. (1999). "High Integrity Carrier Phase Navigation for Future LAAS Using Multiple Civilian GPS Signals." In Proceedings of the *Institute of Navigation GPS 1999 Conference*. Nashville, Tennessee, September 14-17.

Kim, D. and Langly, R. (2003), "On Ultrahigh-precision positioning and navigation: Journal of the Institute of Navigation, Vol. 50, No. 2, pp. 103-116.

Kim, D., and Langley, R. (2000). "GPS ambiguity resolution and validation: Methodologies, trends and issues." *International Symposium on GPS/GNSS.* Seoul, Korea, December 2000.

Klobuchar, J. A., (1996). "Ionospheric Effects on GPS", in *Global Positioning System: Theory and Applications*, edt. B. W. Parkinson and J. J. Spilker, vol.1, ch.12, p.485-514.

Komjathy, A. (1997). "Global ionospheric total electron content mapping using the global positioning system." Ph.D. dissertation, Department of Geodesy and Geomatics Technical Report No. 188, University of New Brunswick, Fredericton, New Brunswick, Canada, 248pp.

Lachapelle,G., M. Cannon, and S. Phalke (2006). "SimGNSSII™ Operating Manual Version 2- Draft." Department of Geomatics Engineering, University of Calgary, Calgary AB, Canada.

Langley, R. B. (1998). "Propagation of the GPS signals." Chapter 3 *GPS for Geodesy*, J.P. Teunisson and A. Kleusberg, Springer-Verlag, Berlin *pp* 111-143.

Leandro, R.F., M.C. Santos and R.B. Langley (2006). "UNB Neutral Atmosphere Models: Development and Perfromance." Proceedings of ION NTM 2006, pp. 564-573, Monterey, California, January 2006.

Misra, P., and P. Enge (2001). *Global positioning system : signals, measurements and performance*. Ganga-Jamuna Press, Lincoln, Mass.

Luo, N. (2001) *Precise Relative Positioning of Multiple Moving Platforms Using GPS Carrier Phase Observables*, Ph.D. thesis, UCGE Report No. 20147, University of Calgary, pp.217.

Odjick, D. (2003). "Ionosphere-Free Phase Combinations for Modernized GPS", J. Surv. Engrg. Volume 129, Issue 4, pp. 165-173

Petovello, M. (2006). "Narrowlane: is it worth it?" *GPS Solutions*, Vol. 10, No. 3, pp.187-195.

Radovanoic, R. (2002). "Adjustment of Satellite-Based Ranging Observations for Precise Positioning and Deformation Monitoring." Geomatics Engineering Department, University of Calgary, Ph.D. thesis, UCGE Report No. 20166.

Ray, J.K (2000). "Mitigation of GPS Code and Carrier Phase Multipath Effects using a Multi-Antenna System", Ph.D. thesis, UCGE Report No. 20136, February 2000, University of

Calgary, pp.260.

Richert, T., and N. El-Sheimy (2007). "Optimal linear combinations of triple frequency carrier phase data from future global navigation satellite systems." *GPS Solutions,* Vol. 11, No. 1, pp. 11-19.

Rizos, C., M. Higgins, and S. Hewitson (2005). "New GNSS Developments and their Impact on Survey Service Providers and Surveyors." Proceedings of SSC2005 Spatial Intelligence. *Innovation and Praxis: The National Biennial Conference of the Spatial Sciences Institute.*

Santos, M. (2003). "Honoring the academic life of Petr Vanicek." *Technical Report 218,* Department of Geodesy and Geomatics, University of New Brunswick, Fredericton, Canada, pp.235.

Seeber, G., (1993) *Satellite Geodesy: Foundations, Methods and Applications*. Walter de Gruyter & Co., Berlin, Germany.

Sükeová, L., M. Santos, R. Langley, R. Leandro, O. Nnani, and F. Nievinski (2007). "GPS L2C Signal Quality Analysis." *Proceedings of the 63rd Annual Meeting of the Institute of Navigation,* Cambridge, MA, USA

Teunissen, P. J. G. (1995). "The least-squares ambiguity decorrelation adjustment: a method for fast GPS integer ambiguity estimation." *Journal of Geodesy,* Vol. 70, No. 1-2, pp. 65-82.

Vollath, U., S. Birnbach, H.Landau, J.M. Fraile-Ordoñez, M. Martin-Neira (1998)

"Analysis of Three-Carrier Ambiguity Resolution (TCAR) Technique for Precise Relative Positioning in GNSS-2." In Proceedings of the *Institute of Navigation GPS 1998 Conference*, Nashville, Tennessee, September 15-17.

Wells, D., N. Beck, D. Delikaraoglou, A. Kleusberg, E. Krakiwsky, G. Lachapelle, R. Langley, M. Nakiboglu, K. Schwarz, J. Tranquilla, and P. Vaníček (1986). *Guide to GPS Positioning.* Department of Geodesy and Geomatics Engineering Lecture Note No. 58, University of New Brunswick, Fredericton, New Brunswick, Canada, 291pp.

APPENDIX I: OPTION FILES

```
Option File for SimGNSSII: No ERRORS

System (GPS, GAL, GPS+GAL)      : GPS

GPS Week                    : 1443
GPS Time To Start (s)          : 0
GPS Time To End (s)            : 10800
Output Interval (s)            : 1

Satellites
  Mask Angle (deg)             : 5
  SV Reject Number             : 0
  SV Rejected                  : 0 0 00 00 00 00
  Ephemeris Type(CANNON/RINEX): CANNON
  Observation Type(CANNON_L1L2CL5/CANNON/RINEX): CANNON_L1L2CL5

Users
Num of Users                   : 1
User Trajectory Interval       : 1
User CoorSys                   : 0
User Trajectory File Name      : TestTrajectory1.txt
User Trajectory File Name      : TestTrajectory2.txt

User Initial Position (Id/Lat(deg)/Lon(deg)/Alt(m))
                          user 1
User Initial Position Lati     : 45.950209098
User Initial Position Longi    : -66.641704745
User Initial Position Height   : 22.7400

Test Area
Test Area (E-W Km)             : 500
Test Area (N-S Km)             : 500
[Centre of Simulated Area]
Latitude  (deg)                : 45.950209098
```

```
Longitude (deg)              : -66.641704745
Altitude  (m)                : 22.7400

Errors
Orbit     Scale Factor       : 0
Iono SPHA Coefficient File Name : gimsSPHAcoef_AprilJune.dat
Iono      Scale Factor       : 0
Iono Frequency Scale Factor  : 0
Trop      Scale Factor       : 0
Average Temperature (deg)    : 20
Relative Humidity            : 0.3
Pressure                     : 1013
MultiPath Scale Factor       : 0.0
Receiver Noise Scale Factor  : 0.0
Code Noise SF for GPS L1     : 0.0
Code Noise SF for GPS L2     : 0.0
Code Noise SF for GPS L5     : 0.0
Carrier Noise SF for GPS L1  : 0.0
Carrier Noise SF for GPS L2  : 0.0
Carrier Noise SF for GPS L5  : 0.0
Code Noise SF for Galileo E1 : 0.0
Code Noise SF for Galileo E2 : 0.0
Code Noise SF for Galileo E3 : 0.0
Carrier Noise SF for Galileo E1 : 0.0
Carrier Noise SF for Galileo E2 : 0.0
Carrier Noise SF for Galileo E3 : 0.0

Cycle Slips (3 modes 0:No 1:Auto 2:User Define)
Cycle Slips Modes            : 0
User Cycle Slips File Name   : CycleSlips1.txt
User Cycle Slips File Name   : CycleSlips2.txt

ALMANAC
GPS ALMANAC(YUMA Format)     : Yuma419.txt
```

```
Option File for SimGNSSII NOISE

System (GPS, GAL, GPS+GAL)   : GPS

GPS Week                     : 1443
GPS Time To Start (s)        : 0
GPS Time To End (s)          : 10800
Output Interval (s)          : 1

Satellites
```

```
  Mask Angle (deg)            : 5
  SV Reject Number            : 0
  SV Rejected                 : 0 0 00 00 00 00
  Ephemeris Type(CANNON/RINEX): CANNON
  Observation Type(CANNON_L1L2CL5/CANNON/RINEX): CANNON_L1L2CL5

Users
Num of Users                  : 1
User Trajectory Interval      : 1
User CoorSys                  : 0
User Trajectory File Name     : TestTrajectory1.txt
User Trajectory File Name     : TestTrajectory2.txt

User Initial Position (Id/Lat(deg)/Lon(deg)/Alt(m))
                          user 1
User Initial Position Lati    : 45.950209098
User Initial Position Longi   : -66.641704745
User Initial Position Height  : 22.7400

Test Area
Test Area (E-W Km)            : 500
Test Area (N-S Km)            : 500
[Centre of Simulated Area]
Latitude  (deg)               : 45.950209098
Longitude (deg)               : -66.641704745
Altitude  (m)                 : 22.7400

Errors
Orbit     Scale Factor        : 0
Iono SPHA Coefficient File Name : gimsSPHAcoef_JulySept.dat
Iono      Scale Factor        : 0
Iono Frequency Scale Factor   : 0
Trop      Scale Factor        : 0
Average Temperature (deg)     : 20
Relative Humidity             : 0.3
Pressure                      : 1013
MultiPath Scale Factor        : 0.0
Receiver Noise Scale Factor   : 1
Code Noise SF for GPS L1      : 0.3
Code Noise SF for GPS L2      : 0.2
Code Noise SF for GPS L5      : 0.1
Carrier Noise SF for GPS L1   : 0.01
Carrier Noise SF for GPS L2   : 0.01
Carrier Noise SF for GPS L5   : 0.01
Code Noise SF for Galileo E1  : 0.045
Code Noise SF for Galileo E2  : 0.03
Code Noise SF for Galileo E3  : 0.1
```

```
Carrier Noise SF for Galileo E1 : 0.003
Carrier Noise SF for Galileo E2 : 0.003
Carrier Noise SF for Galileo E3 : 0.003

Cycle Slips (3 modes 0:No 1:Auto 2:User Define)
Cycle Slips Modes             : 0
User Cycle Slips File Name    : CycleSlips1.txt
User Cycle Slips File Name    : CycleSlips2.txt

ALMANAC
GPS ALMANAC(YUMA Format)      : Yuma419.txt
```

```
Option File for SimGNSSII NORMAL CONDITIONS

System (GPS, GAL, GPS+GAL)    : GPS

GPS Week                  : 1443
GPS Time To Start (s)     : 0
GPS Time To End (s)       : 10800
Output Interval (s)       : 1

Satellites
  Mask Angle (deg)        : 5
  SV Reject Number        : 0
  SV Rejected             : 0 0 00 00 00 00
  Ephemeris Type(CANNON/RINEX): CANNON
  Observation Type(CANNON_L1L2CL5/CANNON/RINEX): CANNON_L1L2CL5

Users
Num of Users              : 1
User Trajectory Interval  : 1
User CoorSys              : 0
User Trajectory File Name : TestTrajectory1.txt
User Trajectory File Name : TestTrajectory2.txt

User Initial Position (Id/Lat(deg)/Lon(deg)/Alt(m))
                    user 1
User Initial Position Lati    : 45.950209098
User Initial Position Longi   : -66.641704745
User Initial Position Height  : 22.7400

Test Area
Test Area (E-W Km)        : 500
Test Area (N-S Km)        : 500
[Centre of Simulated Area]
```

```
Latitude  (deg)              : 45.950209098
Longitude (deg)              : -66.641704745
Altitude  (m)                : 22.7400

Errors
Orbit     Scale Factor       : 0
Iono SPHA Coefficient File Name : gimsSPHAcoef_JulySept.dat
Iono      Scale Factor       : 3.2
Iono Frequency Scale Factor  : 0
Trop      Scale Factor       : 0.2
Average Temperature (deg)    : 20
Relative Humidity            : 0.3
Pressure                     : 1013
MultiPath Scale Factor       : 1.0
Receiver Noise Scale Factor  : 0.5
Code Noise SF for GPS L1     : 0.3
Code Noise SF for GPS L2     : 0.2
Code Noise SF for GPS L5     : 0.0
Carrier Noise SF for GPS L1  : 0.002
Carrier Noise SF for GPS L2  : 0.002
Carrier Noise SF for GPS L5  : 0.002
Code Noise SF for Galileo E1 : 0.045
Code Noise SF for Galileo E2 : 0.03
Code Noise SF for Galileo E3 : 0.1
Carrier Noise SF for Galileo E1 : 0.003
Carrier Noise SF for Galileo E2 : 0.003
Carrier Noise SF for Galileo E3 : 0.003

Cycle Slips (3 modes 0:No 1:Auto 2:User Define)
Cycle Slips Modes            : 0
User Cycle Slips File Name   : CycleSlips1.txt
User Cycle Slips File Name   : CycleSlips2.txt

ALMANAC
GPS ALMANAC(YUMA Format)     : Yuma419.txt
```

```
Option File for SimGNSSII IONOSPHERIC CONDITIONS

System (GPS, GAL, GPS+GAL)   : GPS

GPS Week                     : 1443
GPS Time To Start (s)        : 0
GPS Time To End (s)          : 10800
Output Interval (s)          : 1
```

```
Satellites
  Mask Angle (deg)           : 5
  SV Reject Number           : 0
  SV Rejected                : 0 0 00 00 00 00
  Ephemeris Type(CANNON/RINEX): CANNON
  Observation Type(CANNON_L1L2CL5/CANNON/RINEX): CANNON_L1L2CL5

Users
Num of Users                 : 1
User Trajectory Interval     : 1
User CoorSys                 : 0
User Trajectory File Name    : TestTrajectory1.txt
User Trajectory File Name    : TestTrajectory2.txt

User Initial Position (Id/Lat(deg)/Lon(deg)/Alt(m))
                        user 1
User Initial Position Lati   : 45.950209098
User Initial Position Longi  : -66.641704745
User Initial Position Height : 22.7400

Test Area
Test Area (E-W Km)           : 500
Test Area (N-S Km)           : 500
[Centre of Simulated Area]
Latitude  (deg)              : 45.950209098
Longitude (deg)              : -66.641704745
Altitude  (m)                : 22.7400

Errors
Orbit    Scale Factor        : 0
Iono SPHA Coefficient File Name : gimsSPHAcoef_JulySept.dat
Iono     Scale Factor        : 3.2
Iono Frequency Scale Factor  : 0
Trop     Scale Factor        : 0
Average Temperature (deg)    : 20
Relative Humidity            : 0.3
Pressure                     : 1013
MultiPath Scale Factor       : 0.0
Receiver Noise Scale Factor  : 0.0
Code Noise SF for GPS L1     : 0.0
Code Noise SF for GPS L2     : 0.0
Code Noise SF for GPS L5     : 0.0
Carrier Noise SF for GPS L1  : 0.0
Carrier Noise SF for GPS L2  : 0.0
Carrier Noise SF for GPS L5  : 0.0
Code Noise SF for Galileo E1 : 0.0
Code Noise SF for Galileo E2 : 0.0
```

```
Code Noise SF for Galileo E3    : 0.0
Carrier Noise SF for Galileo E1 : 0.0
Carrier Noise SF for Galileo E2 : 0.0
Carrier Noise SF for Galileo E3 : 0.0

Cycle Slips (3 modes 0:No 1:Auto 2:User Define)
Cycle Slips Modes            : 0
User Cycle Slips File Name     : CycleSlips1.txt
User Cycle Slips File Name     : CycleSlips2.txt

ALMANAC
GPS ALMANAC(YUMA Format)       : Yuma419.txt
```

APPENDIX II: CODE

```
function allPossWidelanes(sys)
%*********************************************************
%*********************************************************
%   Finds all possible widelanes for GPS and Galileo and
%                creates graph
%*********************************************************
%*********************************************************
clc;
c=299792458;%m/s

if strcmpi(sys,'gps')
    f1=1575.42*10^6;
    f2=1227.60*10^6;
    f3=1176.45*10^6;
    lam(1)=c/f1;
    lam(2)=c/f2;
    lam(3)=c/f3;
    im(1)=154;
    im(2)=120;
    im(3)=115;
elseif strcmpi(sys,'gal')
    f1=1575.42*10^6;
    f2=1176.45*10^6;
    f3=1207.14*10^6;
    lam(1)=c/f1;
    lam(2)=c/f2;
    lam(3)=c/f3;
    im(1)=154;
    im(2)=115;
    im(3)=118;
end

q=lam(2)/lam(1);
r=lam(3)/lam(1);
t=lam(3)/lam(2);

div1=gcd(im(1),im(3));%find greatest common denominator

if div1~=1%if gcd is not equal to one divide it to reduce to lowest common
denominator.
    P=im(3)/div1;
else
    P=im(3);%else leave it alone.
end
div2=gcd(im(2),im(3));%find greatest common denominator

if div2~=1%if gcd is not equal to one divide it to reduce to lowest common
denominator.
    R=im(3)/div2;
else
    R=im(3);%else leave it alone.
end
ind_s_i=floor(1-P/2);%define start of index
```

```
ind_e_i=floor(P/2);%define end of index
ind_s_j=floor(1-R/2);%define start of index
ind_e_j=floor(R/2);%define end of index
I=[ind_s_i:1:ind_e_i]';
J=[ind_s_j:1:ind_e_j]';
[i,j]=meshgrid(I,J);
k=ceil(-i*r-j*t);

%plot_widelanes3freq(ind_s_i,ind_e_i,ind_s_j,ind_e_j,lam(3),r,t,'gps')
printResults(i,j,k,sys);


function [i,j,k]=ion_delay_combinations()
%*********************************************************
%*********************************************************
%   Finds all possible widelanes for GPS and Galileo and
%                depending on linearcombinations.m
%                    function which is used
%*********************************************************
%*********************************************************
[i,j,k]=meshgrid([-50:1:50],[-50:1:50],[-50:1:50]);
[lam a b c I_cy I_m N_cy N_m]=linearCombinationsGAL(i,j,k);
ind=find(abs(I_m)<0.01 | abs(I_cy)<0.01);
[s1 s2 s3]=ind2sub(size(i),ind);
i=s2-51;
j=s1-51;
k=s3-51;

[lam a b c I_cy I_m N_cy N_m]=linearCombinationsGAL(i,j,k);


file=['ionreducedL1_L2_L3GAL.dat'];

f1=fopen(file,'w');
fprintf(f1,'i j k A B C lc noise ion noise ion');
fprintf(f1,'\n');
 for q=1:size(i,1)
     if gcd(i(q),j(q))==1 || gcd(i(q),k(q))==1 || gcd(j(q),k(q))==1
           fprintf(f1,'%i %i %i %4.4f %4.4f %4.4f %4.4f %4.4f %4.4f %4.4f
%4.4f',i(q),j(q),k(q),a(q),b(q),c(q),lam(q),N_cy(q),I_cy(q),N_m(q),I_m(q));
           fprintf(f1,'\n');
     end
 end
fclose(f1);
function [i j k]=allPossNR(sys)
%*********************************************************
%*********************************************************
%   Finds all possible noise reduction combinations
%          for GPS and Galileo and creates graph
%*********************************************************
%*********************************************************
clc;
c=299792458;%m/s

if strcmpi(sys,'gps')
```

```
    f1=1575.42*10^6;
    f2=1227.60*10^6;
    f5=1176.45*10^6;
    lam(1)=c/f1;
    lam(2)=c/f2;
    lam(5)=c/f5;
    im(1)=154;
    im(2)=120;
    im(5)=115;
elseif strcmpi(sys,'gal')
    f1=1575.42*10^6;
    f2=1176.45*10^6;
    f5=1207.14*10^6;
    lam(1)=c/f1;
    lam(2)=c/f2;
    lam(5)=c/f5;
    im(1)=154;
    im(2)=115;
    im(5)=118;
end
w=0.0024/0.0019;v=0.0025/0.0019;%noise amplification in meters

x=50;
y=50;
z=50;
i=[0:1:x]';
j=[0:1:y]';
k=[0:1:z]';

[I,J,K]=meshgrid(i,j,k);

[lc lam1 lam2 lam5]=wavelength(I,J,K,sys);

a=I.*lc./lam1;
b=J.*lc./lam2;
c=K.*lc./lam5;

n_m=sqrt(a.^2+b.^2*w^2+c.^2*v^2);%noise amplification metres

ind=find(lc>0.05);

a=1;
[s1 s2 s3]=ind2sub(size(lc),ind);
for w=1:size(s1,1)
     if n_m(s1(w), s2(w), s3(w))<1
        n1(a)=s1(w);
        n2(a)=s2(w);
        n3(a)=s3(w);
        a=a+1;
    end
end
ind2=sub2ind(size(n_m),n1',n2',n3');
i=n2-1;
j=n1-1;
k=n3-1;
```

```
printResultsNR(i',j',k',sys);
%*********************************************************
%*********************************************************
%   Finds all optimal combinations based on criteria
%   for GPS and Galileo depending on linearcombination.m
%               function used
%*********************************************************
%*********************************************************
close all;
clear;
clc;
cc=299792458;%speed of light
f1=1575.42*10^6;f2=1227.60*10^6;f5=1176.45*10^6;
q=f1/f2;r=f1/f5;
lam1=cc/f1;lam2=cc/f2;lam5=cc/f5;

[I,J,K]=meshgrid(-20:1:20,-20:1:20,-20:1:20);

[lam A1 B1 C1 I_cy I_m N_cy N_m MP_cy MP_m]=linearCombinations(I,J,K);
ind=find(10>lam & lam>0.1 & N_m<4 & I_m<0.05 & I_m>-0.05);
[x,y,z]=ind2sub(size(lam),ind);
for w=1:size(x,1)
    i(w,1)=I(x(w),y(w),z(w));
    j(w,1)=J(x(w),y(w),z(w));
    k(w,1)=K(x(w),y(w),z(w));
end
[lam a b c I_cy I_m N_cy N_m MP_cy MP_m]=linearCombinations(i,j,k);
file='optcombinations.txt';
f1=fopen(file,'w');
fprintf(f1,'i j k A B C lc noise ion mp noise ion mp');
fprintf(f1,'\n');
for w=1:size(i,1)
    if gcd(i(w),j(w))==1 || gcd(i(w),k(w))==1 || gcd(j(w),k(w))==1
        fprintf(f1,'%i %i %i %4.4f %4.4f %4.4f %4.4f %4.4f %4.4f %4.4f
%4.4f %4.4f %4.4f
%4.4f',i(w),j(w),k(w),a(w),b(w),c(w),lam(w),N_cy(w),I_cy(w),MP_cy(w),N_m(w)
,I_m(w),MP_m(w));
        fprintf(f1,'\n');
    end
end
fclose(f1);
function [i j k lam N_cy MP_cy I1_cy I2_cy I3_cy N_m MP_m I1_m I2_m
I3_m]=linearCombinations(i,j,k)
%*********************************************************
%*********************************************************
%  Determines the properties of GPS/GAL lienar combinations
%*********************************************************
%*********************************************************
cc=299792458;%speed of light
f1=1575.42*10^6;%frequency on L1
f2=1227.60*10^6;%frequency on L2
f5=1176.45*10^6;%frequency on L5
f1=1575.42*10^6;%frequency on E1
f2=1176.45*10^6;%frequency on E5a
f5=1207.14*10^6;%frequency on E5b
```

```
w=0.0024/0.0019;v=0.0025/0.0019;%noise amplification in meters
x=0.0099/0.010;y=0.0099/0.010;%noise amplification in cycles

lam1=cc/f1;%wavelength L1
lam2=cc/f2;%wavelength L1
lam5=cc/f5;%wavelength L1

f=i.*f1+j.*f2+k.*f5;%LC frequency
lam=(lam1.*lam2.*lam5)./(i.*lam2.*lam5+j.*lam1.*lam5+k.*lam1.*lam2);%LC
wavelength

a=i.*lam./lam1;
b=j.*lam./lam2;
c=k.*lam./lam5;

I1_cy=(i+(f1/f2).*j+(f1/f5).*k);%1st order ionospheric delay amplification
in cycles
I2_cy=(i+(f1/f2)^2.*j+(f1/f5)^2.*k);%2nd order ionospheric delay
amplification in cycles
I3_cy=(i+(f1/f2)^3.*j+(f1/f5)^3.*k);%3rd order ionospheric delay
amplification in cycles


I1_m=(a+b.*(f1/f2)^2+c.*(f1/f5)^2);%1st order ionospheric delay
amplification in meters
I2_m=(a+b.*(f1/f2)^3+c.*(f1/f5)^3);%2nd order ionospheric delay
amplification in meters
I3_m=(a+b.*(f1/f2)^4+c.*(f1/f5)^4);%3rd order ionospheric delay
amplification in meters

N_cy=sqrt(i.^2+x^2*j.^2+y^2*k.^2);%noise amplification cycles
N_m=sqrt(a.^2+b.^2*w^2+c.^2*v^2);%noise amplification metres

mp1=1/4;
mp2=1/4;
mp5=1/4;
MP_cy=abs(i)*mp1+abs(j)*mp2+abs(k)*mp5;
MP_m=(abs(a)+(f1/f2).*abs(b)+(f1/f5).*abs(c));

%A={'lambda' 'ion1cy' 'ion2cy' 'ion3cy' 'ion1m' 'ion2m' 'ion3m' 'N_cy'
'N_m' 'MP_cy' 'MP_m';...
%   num2str(lam) num2str(I1_cy) num2str(I2_cy) num2str(I3_cy) num2str(I1_m)
num2str(I2_m) num2str(I3_m) num2str(N_cy) num2str(N_m) num2str(MP_cy)
num2str(MP_m)}
```